Remarks

Claims 37-40, 58 and 61 have been amended. Support for this amendment is found in the specification at least on page 2, lines 12-13 of the specification. Claims 1-36, 41-57 and 59-60 have been cancelled. Claims 31-36, 41-57 and 59-60 are cancelled herein for being drawn to non-elected subject matter and Applicants understand that these claims may be pursued in subsequent divisional applications without prejudice. By entry of this amendment, claims 37-40, 58 and 61 are pending.

Claims 38-40, 58 and 61 erroneously mixed up SEQ ID NO:2 and SEQ ID NO:3 and have been amended to provide correct reference to the sequence identifiers corresponding to the human and murine DIO-1 polypeptide sequences. This amendment is typographical and does not incorporate new matter or require further search.

Sequence Listing

Applicants have provided a corrected version of the sequence listing, in paper copy and CRF, containing all sequences in the specification and conforming to 37 CFR 1.821(e-f) or 1.825(b) or 1.825(d). Please replace the sequence listing after the abstract of the specification with the corrected version submitted herewith. The specification is amended to provide correct sequence identifiers for all sequences in the sequence listing.

Statement under 37 CFR 1.821(e-f) or 1.825(b) or 1.825(d)

The content of the paper and computer readable sequence listings are identical to each other and do not include new matter that extends beyond the content of the originally filed application.

Rejections under 35 U.S.C. §101

Claim 61 is rejected under 35 U.S.C. §101 as being directed to non-statutory subject matter. Applicants traverse the rejection as applied to the claims as amended.

Claim 61 has been amended to recite an *isolated* polypeptide. Applicants respectfully request withdrawal of this rejection.

Rejections under 35 U.S.C. §112, second paragraph

Claim 61 is rejected under 35 U.S.C. §112 as being indefinite. Applicants traverse the rejection as applied to the claims as amended.

Claim 61 has been amended to recite an isolated polypeptide for use as a medicament comprising SEQ ID NO:3 or SEQ ID NO:4. This claim is clear and definite. Applicants respectfully request withdrawal of this rejection.

Rejections under 35 U.S.C. §112, first paragraph (written description)

Claims 37-39, 58 and 61 have been rejected under 35 U.S.C. §112 as lacking written description. Applicants traverse the rejection as applied to the claims as amended.

Claims 37-39 have been amended to recite that the variants and alleles are functionally equivalent to the sequences shown in SEQ ID NO:3 and SEQ ID NO:4. These amendments render the claims clear and teach the invention sufficiently to the skilled person. The originally filed application states that the 'terms "variants" and "alleles" means that they are derived from the sequences given in the figures and have the same function as those'. (Page 2, lines 12-13).

The skilled person would understand that applicants are claiming only functional variants and alleles of the listed sequences. The skilled artisan would be able to visually examine a sequence to determine whether it is likely to be functional or non-functional and can routinely

test suitable candidates using the methods described in Example 3 of the specification to see if they are functional. As an extreme example, an amino acid or DNA sequence which is 95% similar to one of the listed sequences is very likely to demonstrate the same function, likewise an amino acid or DNA sequence which is only 5% similar to one of the listed sequences is very unlikely to demonstrate the same function. Each residue of a sequence may be mutated in one or more ways and the skilled artisan appreciates that some mutations may be 'silent' (i.e. have no effect on the function of the sequence) whereas others may enhance, decrease or eliminate the function of a sequence. The skilled artisan would be able to predict, with reasonable accuracy, which mutations are likely to affect the function of the sequence. With respect to the argument that 'the skilled man cannot envision the detailed structure of the encompassed polynucleotides, polypeptides, or variants thereof', the skilled person routinely uses simple publicly available bioinformatics software to translate nucleotide sequences to amino acid sequences and *vice versa*. One example of suitable software is the 'backtranseq' available within the EMBOSS suite of software which may be accessed at http://www.rfcgr.mrc.ac.uk/Software/EMBOSS/Apps/backtranseq.html. The specification clearly provides sufficient information to allow persons of ordinary skill in the art to repeat the claimed invention.

Rejections under 35 U.S.C. §112, first paragraph (enablement)

Claims 58 and 61 have been rejected under 35 U.S.C. §112 for failing to comply with the enablement requirement. Applicants traverse the rejection as applied to the claims as amended.

Claims 58 and 61 are directed to an isolated polypeptide of SEQ ID NO:3 or SEQ ID NO:4 for use as a medicament. Please argue that the *in vitro* experiments are representative of

the *in vivo* situation and (b) the skilled man would readily be able to create a pharmaceutical composition comprising SEQ ID NO:3 or NO:4 without undue inventive or experimental effort.

Although much of the work disclosed in the specification concerns *in vitro* studies, part of the work has been carried out in an *in vivo* model (chicken limbs) thereby providing an actual reduction to practice of the claimed invention (*See* Example 6 on page 9 of the specification). These experiments have also been published further supporting the in vivo actions of these proteins. (*See* Figure 5 of Garcia-Domingo *et al.*, *PNAS USA* 1999, 96 pp 7992-7997). A skilled person could easily repeat the invention using the information disclosed in the patent application and his general scientific knowledge. Also, the Garcia-Domingo *et al* papers (1999 and 2003 - enclosed) provide details of methods used. Although these papers were published after the filing date of the present application, they report work carried out before the filing date and therefore demonstrate that the skilled man was able to carry out such procedures at the relevant time.

Furthermore, the Examiner remarks that *in vitro* experiments do not adequately predict *in vivo* outcomes due to the loss of phenotypic characteristics associated with their normal counterpart cell type (Culture of Animal Cells, A Manual of Basic Technique, Alan R.Liss Inc. 1983, New York). Such loss of phenotypic characteristics is due to the increased survival potential of long-term cultured cells, and mainly concerns the loss of response to apoptotic stimuli, for example loss of the pro-apoptotic protein p53 (The role of p53 and pRB in apoptosis and cancer, Hickman *et al.*, *Current Opinion in Genetics & Development*, 2002, 12:1, pp 60-66). The pending claims are directed to exactly the response to apoptotic stimuli that would <u>not</u> favour the increased survival potential of cultured cells, and it is safe to assume that the same response is not an acquired feature of the cultured cells, and will also be present *in vivo*. Applicants submit that the Hickman paper is just one example taken from many others which

demonstrates that in the present case that the *in vitro* situation is predictive of the *in vivo* situation.

Rejections under 35 U.S.C. §102

Claims 37-39 and 61 have been rejected under 35 U.S.C. §102(b) as being anticipated by Nagase et al. (*DNA Research* 1997; 4(2):pp141-150). Applicants traverse the rejection as applied to the claims as amended.

The Examiner states on page 13 of the Office Action that a sequence comparison is attached. Applicants can find no sequence comparison attached the the Office Action nor does Nagase *et al* (1997) provide a sequence comparison. Therefore, Applicants have used publicly available software to identify the open reading frame of nucleotide SEQ ID NO:1 and aligned this open reading frame (*i.e.* amino acid SEQ ID NO:3) with the polypeptide KIAA0333 identified by Nagase *et al* to produce alignment 1 in the same manner that one of ordinary skill in the art would use. This procedure was repeated for SEQ ID NO: 4 to produce alignment 2. The alignment software is available at http://prodes.toulouse.inra.fr/multalin/multalin.html. Copies of the alignments are enclosed as exhibits to the following discussion.

Alignment 1 (KIAA0333 vs SEQ ID NO:3)

KIAA0333 is 991 amino acids long whereas SEQ ID NO:3 is 562 amino acids long. The alignment does not provide coordinates for each of the sequences, therefore we provide the following table to clarify matters.

Alignment Numbering	Equivalent numbering for:		Comment
	SEQ ID NO: 3	KIAA0333	
1-234	1-234	(none)	SEQ ID NO: 3 starts upstream of KIAA0333
235-387	235-387	1-153	Identical
401-413	(gap)	154-166	Gap in SEQ ID NO: 3 sequence
414-565	387-538	167-317	Identical
565-598	539-562	318-350	Not similar
599-1226	(none)	351-991	KIA0333 continues downstream of end of SEQ ID NO: 3

The predicted N terminus of SEQ ID NO:3 lies 234 amino acid residues upstream of the predicted N terminus of the KIAA0333 polypeptide. Although residues 235-387 of SEQ ID NO:3 are identical to the first 153 residues of KIAA0333, the subsequent 36 residues of KIAA0333 are not present in SEQ ID NO: 3 and a gap is observed in the alignment. This gap is followed by a region of 151 residues which are identical in SEQ ID NO: 3 (i.e. residues 387-538) and KIAA0333. The final 33 residues (i.e. residues 529-562) of SEQ ID NO: 3 show no similarity with KIAA0333.

If the skilled person was presented with the nucleotide or amino acid sequence of Nagase *et al* he would need to carry out extensive bioinformatic and laboratory experimentation in order to identify SEQ ID NO: 3.

For a prior art reference to anticipate a claim, the prior art reference must disclose all elements of the claim and also be an enabling disclosure. Nagase gives no indication that if expressed, his nucleotide sequences would provide a functional DIO-1 protein. If the information provided in Nagase was taken at face value, an attempt to express the polypeptide described would likely fail. In the unlikely event that a polypeptide was expressed, it is likely that the polypeptide would not fold properly (due to a lack of correct folding signals within the sequence) and would therefore be degraded by 'quality control' proteases. Even if a functional

protein were to be produced from the KIAA0333 DNA, it is unlikely that the resultant protein would have the same, or even similar, function to that of the polypeptide encoded by SEQ ID NO:1. Although both sequences encode a Zinc Finger motif, only SEQ ID NO:3 encodes a glutamine rich region, an acidic transcriptional activating domain and a nuclear localisation signal. Therefore, we submit that KIA0333 is not a functional allele or functional variant of the polypeptide encoded by SEQ ID No.1.

We also submit that disclosed KIAA0333 sequences would not inspire the skilled man to identify SEQ ID NO: 1 or 3.

The predicted KIAA0333 polypeptide is not encoded by any of the usual ATG start codon. The skilled artisan would understand that not all genes are expressed by an organism, therefore there would be no guarantee that a protein would ever be produced from a DNA sequence. Nagase does not supply the upstream nucleotide region and it is impossible to look for possible ribosome binding sites from this sequence. Therefore, it is highly unlikely that the skilled man would predict the KIAA0333 nucleotide sequence to encode any polypeptide, let alone the one disclosed in SEQ ID NO: 3. Even if the skilled artisan did take a somewhat unusual step and decide to study KIAA0333, he would need to carry out undue bioinformatic and laboratory experimentation to identify the upstream nucleotide region. It would be neccesary to identify a putative start codon and appropriately located ribosome binding site before a sequence would suggest that it might encode a protein. The skilled artisan would then have to carry out 'primer extension' analysis in order to identify a promoter for the putative gene - such analysis is time consuming and requires a good amount of practical skill. If a promoter region was identified then the skilled man would be reasonably (but not 100%) sure that this putative gene encoded a

protein. As such, Nagase does not provide an enabling disclosure to anticipate functional variants or alleles of SEQ ID NO:3.

Alignment 2 (KIAA0333 vs SEQ ID NO:4)

Similarly, there are large discrepancies between KIAA0333 and SEQ ID NO:4. The similarity between KIAA0333 and SEQ ID NO:4 is considerably lower than the similarity between KIAA0333 and SEQ ID NO:3. For the same reasons presented above, Applicants submit that Nagase *et al* neither teaches nor inspires the skilled man to identify SEQ. ID NO: 4.

Claim Objections

Claim 40 is objected to as being dependent upon a rejected base claim. This claim has been rewritten in independent form including all of the limitations of the base claim.

Conclusion

Applicants submit that the pending claims define novel and patentable subject matter and provide a complete response to the Office Action. Accordingly, Applicants respectfully request allowance of these claims. No additional fees are believed due, however, the Commissioner is hereby authorized to charge any deficiencies which may be required, or credit any overpayment, to Deposit Account Number 11-0855.

Early and favorable consideration is earnestly solicited. If the Examiner believes any informalities remain in the application that can be resolved by telephone interview, a telephone call to the undersigned attorney is earnestly solicited.

Respectfully submitted,

Robert E. Richards, Esq.
Reg. No.- 29,105

KILPATRICK STOCKTON LLP
1100 Peachtree Street
Suite 2800
Atlanta, Georgia 30309-4530
Tel. (404) 815-6500
Docket No : 46309-253995 (23890)

The role of p53 and pRB in apoptosis and cancer

Emma S Hickman, M Cristina Moroni and Kristian Helin*

Loss of function of both the p53 pathway and the retinoblastoma protein (pRB) pathway plays a significant role in the development of most human cancers. Loss of pRB results in deregulated cell proliferation and apoptosis, whereas loss of p53 desensitises cells to checkpoint signals, including apoptosis. In the past two years, mouse genetics and gene expression profiling have led to major advances in our understanding of how the pRB and p53 pathways regulate apoptosis and thus the development of tumours.

Addresses
European Institute of Oncology, Department of Experimental Oncology, Via Ripamonti 435, 20141 Milan, Italy
*e-mail: khelin@ieo.it

Current Opinion in Genetics & Development 2002, 12:60–66

0959-437X/02/$ – see front matter

Abbreviations

ATM	ataxia telangiectasia mutated
ATR	ATM related
bHLH	basic helix–loop–helix
CDK	cyclin-dependent kinase
CNS	central nervous system
MEF	mouse embryo fibroblast
PNS	peripheral nervous system
pRB	retinoblastoma protein

Introduction

The *TP53* and *RB1* tumour suppressor genes are frequent targets of mutation during tumorigenesis. The *TP53* gene product, p53, guards against genomic instability and oncogene expression by inducing both arrest of the cell cycle and apoptosis. In contrast, the retinoblastoma protein (pRB) regulates apoptosis during development, and its loss results in deregulated growth and apoptosis. In the latter case, suppression of apoptosis is required for tumours to develop.

In this review, we focus on the most recent advances in our understanding of the functions of these two genes, with emphasis on their respective roles in apoptotic pathways.

The p53 tumour suppressor

The importance of the *TP53* gene in suppressing tumour development is illustrated by the fact that it is disrupted in roughly 50% of all human tumours. Mouse models have shown that although p53 function is basically dispensable for embryonic development and normal progression of the cell cycle, p53 null mice are susceptible to lymphomagenesis, which results in an average lifespan of 5 months [1,2]. In fact, p53 governs an essential growth checkpoint that both protects against genomic rearrangement or the accumulation of mutations, and suppresses cellular transformation caused by oncogene activation or the loss of tumour suppressor pathways (for reviews, see [3] and Michael and Oren, this issue [pp 53–59]).

Figure 1

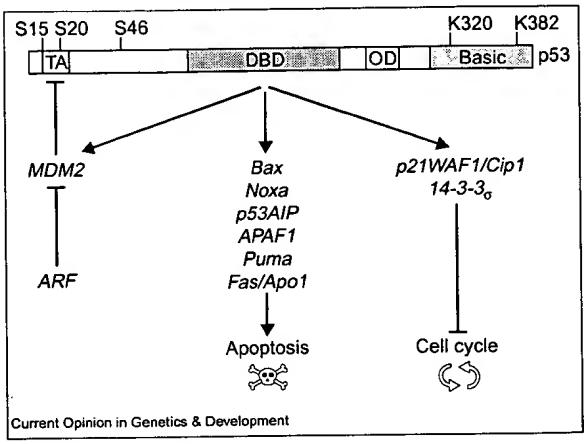

Summary of p53 function and regulation. From the amino to the carboxyl terminus, the functional domains of p53 include the transactivation/transrepression domain (TA), the DNA-binding domain (DBD), the oligomerisation domain (OD), and the basic allosteric control region (Basic). Arrows indicate p53-transactivated genes and the downstream effects of their expression. Bars represent repression. Some of the sites of p53 phosphorylation (serines 15, 20 and 46) and acetylation (lysines 320 and 382) are also indicated.

Levels of p53 are normally low owing to the short half-life of the protein; however, both intracellular and extracellular stress signals can induce the stabilisation and activation of p53, albeit via different mechanisms. DNA-damaging agents, such as ultraviolet or γ irradiation and chemotherapeutic drugs, stabilise and activate p53 by covalent modification (for reviews, see [4,5] and Bulavin *et al.* [pp 92–97] in this issue). This involves phosphorylation of the transactivation domain, and both acetylation and phosphorylation of the basic allosteric control region (Figure 1).

Recently, the identification of the kinases involved in p53 activation has been the focus of intense study. Notably, the ATM (ataxia telangiectasia mutated) and ATR (ATM related) kinases phosphorylate p53 after ionising radiation and ultraviolet irradiation, respectively. Consequently, cells that lack expression of either of these genes or their other known substrates, CHK1 and CHK2 (which also phosphorylate p53), display reduced stabilisation and activation of p53 in response to these DNA-damaging agents [6–8]. Thus, it is now clear that different stress signals induce p53 through different pathways, and the mediators of these pathways are beginning to emerge.

p53 may also be stabilised and activated by internal aberrations such as the deregulation of cellular oncogenes. Overexpression of some oncogenes induces expression of $p14/19^{ARF}$ (hereafter called ARF), which by inactivating

MDM2 blocks degradation of p53 (see review by Michael and Oren in this issue [pp 53–59]). Once activated, p53 can induce either cell-cycle arrest or apoptosis. After DNA damage, p53 expression blocks progression of the cell cycle until the DNA can be repaired; alternatively, if the damage is extensive, the cells enter into apoptosis. However, the exact outcome of p53 induction may be cell-specific and dependent on both the type and the strength of the stimulus. Furthermore, cells that overexpress oncogenes or that have lost tumour suppressor pathways frequently express high levels of p53 and are abrogated in their ability to establish cell-cycle arrest. Consequently, tumour cells are generally much more sensitive to DNA-damaging agents than their primary counterparts — a fact that forms the conceptual basis of chemotherapy.

Mechanisms of p53-induced apoptosis

By far the best characterised function of p53 is that of a transcription factor, mediating both transactivation and transrepression of target genes. Many of the genes regulated by p53 have been shown to participate in apoptotic pathways (Table 1); however, many features of the mechanism underlying p53-mediated apoptosis remain unresolved. For example, although all of the genes in Table 1 have been shown to be required for p53-mediated apoptosis in some cell systems, no single target gene has been identified as pivotal to the apoptotic pathway. Moreover, although transactivation is required for the growth arrest function of p53, it is less clear whether the transactivation and transrepression functions of p53 are required for induction of apoptosis. A p53 mutant that cannot activate or repress transcription has been shown to be both functional and deficient in the induction of apoptosis, depending on the cell-culture system used (see [9•] and reference therein).

Two major drawbacks in p53 mutant studies have been the limited number of cell types used and the non-physiological levels of p53 expression. To circumvent these problems, two groups have constructed embryonic stem cells and mice in which the wild-type p53 has been replaced with a transactivation- and transrepression-deficient mutant of p53 [9•,10•]. These groups report that mutant embryonic stem cells and thymocytes are resistant to γ-irradiation-induced apoptosis, that mutant mouse embryo fibroblasts are transformed by oncogenes, and that the mice are prone to developing tumours. Taken together with the observation that the expression levels of p53-activated and -repressed genes do not change after DNA damage in the mutant cells, these results strongly suggest that an intact p53 transactivation domain is required for p53-dependent apoptosis.

Activated p53 regulates the expression of several apoptotic mediators including members of the Bcl-2 and TNF receptor families (Table 1). The pro-apoptotic BH3 domain protein, Bax, was the first apoptotic factor to be identified as a target for p53 transactivation [11,12]. Interestingly, the same studies also showed that p53 represses the expression of Bcl-2 and thereby contributes to apoptosis by blocking survival signals mediated by Bcl-2 [11,12]. Subsequently, the death receptor ligand Fas/apo1 was shown to be induced by p53, suggesting that p53 may also induce caspase activation through death receptor signalling [13]. SAGE analysis of cells that overexpress p53 has identified a separate class of p53-induced genes, or 'PIGs', that may initiate apoptosis by regulation of cellular redox potential [14].

Table 1

List of proapoptotic p53 target genes.

Gene(s)	Act/Repr.	Gene function	Reference(s)
Bax	A	Mitochondrial pore protein	[11,12]
Fas/Apo1	A	Death receptor ligand	[13]
Killer/DR5	A	Death receptor	[54]
PIG3	A	Redox regulation	[14]
PUMA	A	Pro-apoptotic BH3 protein	[15•,16•]
NOXA	A	Pro-apoptotic BH3 protein	[17•]
NF-κB	A	Transcription factor	[18•]
p53AIP	A	Dissipates mitochondrial potential	[19•]
APAF1	A	Procaspase 9 activation	[22•]
PIDD	A	Death domain protein	[20•]
p53DINP1	A	p53 phosphorylation at Serine 46	[24•]
PERP	A	Pro-apoptotic transmembrane protein	[26•]
Bcl2	R	Anti-apoptotic BH3 protein	[11]

Cell cycle regulated genes have been omitted for simplicity. Both p53 activated genes (A) and one repressed gene (R) are listed.

The past two years have witnessed the identification of several novel p53-regulated genes. The list includes genes encoding two BH3 domain proteins, PUMA [15•,16•] and NOXA [17•], that associate with anti-apoptotic Bcl-2 family proteins and promote release of cytochrome *c*. Other new p53 targets include NF-κB, a mediator of TNF receptor signalling [18•]; p53AIP, which dissipates mitochondrial potential by an unknown mechanism [19•]; and PIDD, a novel death domain protein that participates in death receptor signalling [20•]. Furthermore, *APAF1*, which encodes an adaptor protein that enables the cytochrome-*c*-dependent activation of procaspase 9 [21], has been identified as a direct transcriptional target of p53 and the transcription factor E2F ([22•]; and see below).

All of these genes have been shown to be required for apoptosis in at least some cell systems and it seems that their relative importance in the p53 response is likely to be specific to the cell type. In coming years it will be interesting to establish whether any of these genes function as tumour suppressors themselves, as has been shown recently for *APAF1* in the development of melanoma [23••]. The loss of such tumour suppressors may be linked to the low frequency of p53 mutation in certain types of tumour.

An emerging concept in our understanding of p53 is that 'active p53' is a protein that is subject to differential covalent

modification, and it appears that these modifications markedly influence the expression of target genes. Evidence for this has been provided by a few recent studies.

First, the induction of the pro-apoptotic p53-target *p53AIP* was shown to coincide temporally with phosphorylation of p53 at serine 46 and was only achieved as a consequence of severe DNA damage [19•]. The data suggest that there is a phosphoserine-46-dependent switch between the initial expression of cell-cycle inhibitory genes and the subsequent expression of pro-apoptotic p53 target genes. The p53 target gene *p53DINP1* was shown to be necessary for both phosphorylation of serine 46 and apoptosis, which suggests that the p53DINP1 protein may be involved in the process by which the p53 response is regulated temporally [24•].

Second, treatment with DNA-damaging agents that activate different pathways and phosphorylate p53 at different sites also induce differential gene expression [25•]. Two other groups have reported that the pro-apoptotic p53 target genes *PERP* and *Pw1/Peg3* are specifically induced in cells undergoing apoptosis [26•,27]. Whether these differences reflect phosphorylation-induced conformational change in p53, or differential gene expression is achieved through interaction with different cofactors remains to be established.

The retinoblastoma protein

Genetic and biochemical data have placed pRB in a linear pathway that is deregulated in most human cancers (for reviews, see [28,29]). This pathway includes both cyclin-dependent kinase (CDK) inhibitors of the INK4 family of proteins, which are negative regulators of cell proliferation, and the positively acting D-type cyclins that form active kinase complexes in association with CDK4 or CDK6. CDKs phosphorylate pRB, which abolishes its activity. The activity of the CDKs, and therefore of pRB, is regulated by external mitogenic and anti-mitogenic factors. It is currently thought that inactivation of the pRB pathway is an obligatory step in cancer that renders cells insensitive to anti-mitogenic signals [30].

The *RB1* gene was the first mammalian tumour suppressor gene to be isolated. Germline mutations in *RB1* are associated with childhood retinoblastomas and a predisposition to osteosarcomas [31]. In contrast, somatic mutations in *RB1* contribute to the development of several human tumours, including retinoblastomas, osteosarcomas, lung carcinomas, renal cell carcinomas and bladder carcinomas. These observations have raised the following question: why do germline *RB1* mutations result in a predisposition to retinoblastomas and osteosarcomas, and not to the wide spectrum of cancers in which inactivation of pRB is essential?

Although this question is still being investigated, one plausible answer has been found in the observation that in most cells apoptosis is the outcome of loss of pRB. Therefore, other genetic alterations are required to prevent apoptosis in a pRB-deficient cell. In this perspective, retinal cells and osteoblasts are unusual, because these cells tolerate loss of pRB for a period of time without other genetic alterations — perhaps owing to survival signals from surrounding cells. The frequency with which the pRB pathway is deregulated in human cancer, together with the observation that lack of pRB results in apoptosis, have led investigators to study the mechanism by which pRB regulates apoptosis.

Regulation of apoptosis by pRB

Mouse genetic data have pointed to a physiological role of pRB in the regulation of apoptosis [29]. pRb-deficient mice die during embryogenesis (between embryonic days 13 and 15), displaying extensive apoptosis, ectopic S phase and a lack of differentiation in the central (CNS) and peripheral (PNS) nervous systems, ocular lens and liver. These defects are observed in tissues in which pRb is highly expressed in normal animals [29,32]. Because pRB is activated on exit of the cell cycle during differentiation, it is thought that the function of pRB is to protect differentiating cells from apoptosis.

Recent studies using mice chimaeric for wild-type and pRb-deficient cells showed that the extensive apoptosis and lack of differentiation, but not the ectopic cell cycles, that occur in *Rb−/−* cells were suppressed in chimaeric mice [33•]. On the basis of these results, Lipinski *et al.* [33•] concluded that deregulation of the cell cycle as a result of loss of pRb is a cell-autonomous phenomenon, whereas apoptosis and differentiation are non-cell-autonomous. Although protection of the pRb-deficient cells in the chimaeras was not complete, these results are important conceptually, because they suggest that wild-type cells can send survival signals to pRB-deficient cells during tumorigenesis, perhaps allowing these cells to survive for long enough to acquire other genetic alterations.

The underlying molecular mechanisms by which pRB regulates apoptosis are still under intense investigation. The above results suggest that wild-type cells produce a survival signal that is abolished in pRb-deficient cells; however, no signals in the form of either secreted factors or proteins mediating cell–cell contacts have been characterised. More is known about the cell-autonomous mechanisms through which loss of pRB induces apoptosis.

Early studies noted a strong correlation between loss of pRB and lack of functional p53 in human tumours [28]. Taken together with the fact that several DNA tumour viruses, such as human papilloma viruses, encode proteins that inactivate both pRB and p53, it has been suggested that loss of pRB results in p53-dependent apoptosis. This suggestion was confirmed in mouse embryos lacking p53 and pRb, which showed strong suppression of apoptosis in the CNS and the ocular lens, but not in the PNS [34,35].

Most of the research into the molecular mechanisms by which loss of pRB results in apoptosis has focused on the

best known targets of pRB — the E2F transcription factors (for review, see [36]). Several results suggest that the E2Fs provide a good model for how pRB regulates not only cell proliferation but also apoptosis. Ectopic expression of E2F1, and also other members of the E2F family, has been shown to induce apoptosis in tissue-culture cells and in transgenic mice [22•,36–38] — an effect that is potentiated by the presence of wild-type p53 [36,37]. Furthermore, mutant mouse embryos lacking E2F1 or E2F3 and pRb survive longer than *Rb*$^{-/-}$ embryos, and display a significant reduction of apoptosis and ectopic S phases [39,40•].

It is important to stress that ablation of either *E2f1* or *E2f3* is insufficient to allow *Rb*$^{-/-}$ mice to survive until birth. One explanation for this result may be that redundancy occurs among the E2F transcription factors, and that deletion of more than one E2F is required for *Rb*$^{-/-}$ embryos to survive. An alternative explanation might be that pRB has additional targets and that deregulation of these factors contributes to the phenotype of the *Rb*$^{-/-}$ embryos (see below).

E2F target genes involved in apoptosis

As mentioned above, p53 is required for the apoptosis observed in the CNS and in the eye lens in *Rb*$^{-/-}$ embryos, and also potentiates the apoptosis detected on ectopic expression of E2F. In accord with this, loss of pRB and overexpression of E2F1 both result in increased levels of p53, and a direct link between the two pathways was provided when ARF was identified as a transcriptional target of E2F1 [41,42]. This finding was considered a major breakthrough, because expression of ARF was also known to increase levels of p53 (see review by Michael and Oren in this issue [pp 53–59]). This suggested a relatively simple mechanism in which E2F1-mediated transcriptional activation of *ARF* is linked to apoptosis through increased levels of p53.

Although attractive, this model was too simple. First, loss of pRB and overexpression of E2F1 result in both p53-dependent and p53-independent apoptosis. Second, overexpression of ARF results in growth arrest and not apoptosis [43]. Therefore, the identification of *ARF* as an E2F-regulated gene was not sufficient to explain how loss of pRB induces apoptosis, but it was important conceptually because it provided a link between pRB/E2F and p53. Moreover, because *ARF*$^{-/-}$ mouse embryo fibroblasts (MEFs) have been shown to be more resistant to E2F1-induced apoptosis than wild-type MEFs [44], expression of ARF appears to sensitise fibroblasts to apoptosis.

Two groups reported recently that E2F1 induces transcription of *p73* [45•,46•]. p73 belongs to the p53 family, and shares sequence homology and functional similarity with p53. Unlike ARF, expression of p73 can induce apoptosis, and a dominant-negative p73 mutant can suppress E2F1-induced apoptosis in cells lacking p53. Moreover, induction of apoptosis by E2F1 is severely impaired in *p73*$^{-/-}$ MEFs, and this effect is even more pronounced in

Figure 2

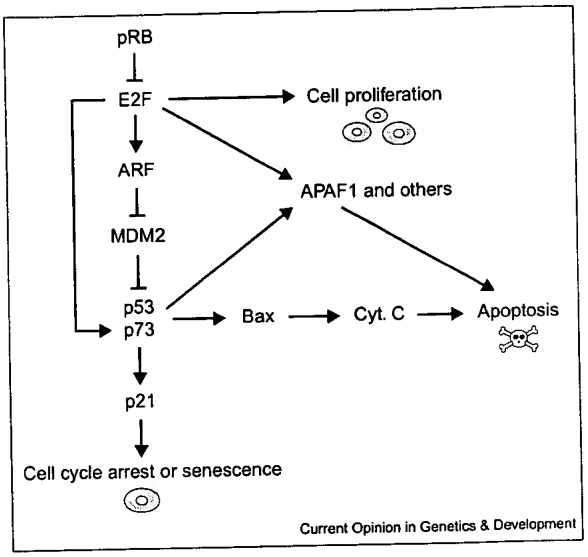

pRB controls proliferation and apoptosis through active repression of E2F-dependent promoters. Apoptosis is regulated through the regulation of cytochrome *c* release (mediated by p53 and/or p73) and through the transcriptional regulation of proapoptotic genes (illustrated here by APAF1). If key players regulating apoptosis and/or cell-cycle arrest are mutated (e.g. ARF, p53, APAF1) or overexpressed (e.g. MDM2), loss of pRB function results in hyperproliferation. In the absence of such alterations, loss of pRB results in growth arrest and/or apoptosis.

MEFs lacking both *p53* and *p73* [45•]. Because p73 might be envisaged as an alternative to p53 in activating mitochondrial dependent apoptosis upon deregulation of the pRB pathway, it would be interesting to determine whether p73 levels are increased in *Rb*$^{-/-}$ embryos. In particular, it will be important to test whether p73 levels are increased in the PNS, which undergoes p53-independent apoptosis, and whether lack of functional p73 suppresses apoptosis in *Rb*$^{-/-}$ embryos.

A recent gene expression analysis has revealed that many potential target genes of E2F may be involved in E2F-mediated apoptosis [47•]. Particularly intriguing was the finding that *APAF1* is a direct target of E2F [22•,47•]. Importantly, APAF1 levels are increased in *Rb*$^{-/-}$ embryos, particularly in the nervous system, and apoptosis in *Apaf1*$^{-/-}$ MEFs is impaired in response to increased E2F1 activity [22•]. Because APAF1 has a central role in stress- and oncogene-induced apoptosis [48], the latter result may not appear surprising. However, a causal role for the regulation of APAF1 by the E2Fs has been suggested by the finding that the ability of E2F1, E2F2 and E2F3 to induce apoptosis correlates with their ability to activate expression of APAF1 [22•].

A model showing how pRB might regulate apoptosis through active repression of E2F-dependent promoters is

presented in Figure 2. Central to this model is the regulation of ARF, p73 and APAF1 levels by E2F, and it is envisaged that increased transcriptional activity of p53 and/or p73 is sufficient to trigger release of cytochrome *c* from the mitochondria. Loss of pRB results in increased levels of APAF1 (and perhaps of some caspases [47•]), which sensitises the pRB-deficient cells to the increased level of cytochrome *c*.

Notably, such a model is consistent with the fact that ablation of any of the key proteins would desensitise the mutated cells to apoptosis. It is important to emphasise, however, that apoptosis induced by loss of pRB may involve more proteins than are depicted here [47•,49], and that the relative importance of each of these proteins may be dependent on the cell type.

Id2 in pRB-regulated apoptosis

The loss of Id2, another pRB-associated protein, has been reported recently to suppress many of the defects observed in pRb-deficient embryos [50••]. *Id2/Rb* double knockout embryos survive to term with no obvious defects in neurogenesis and haematopoiesis, but they die at birth with severe reduction of muscle tissue. Although these results show that there is a genetic interaction between Id2 and pRB, they do not yet explain clearly the biochemical mechanism through which Id2 contributes to such a marked rescue of the phenotype in the pRb-deficient embryos, and thus more experiments are required to clarify this issue. It is important to note, however, that Id2 is an inhibitor of the basic helix–loop–helix (bHLH) class of transcription factors, which are essential for various aspects of cell differentiation during development. The deletion of *Id2* would therefore lead to increased activity of the bHLH transcription factors, resulting in proliferation defects and increased differentiation potential or lack of development.

Consistent with this, proliferation defects and lack of development are observed in several tissues in $Id2^{-/-}$ mice [51,52]. These proliferation defects might be a result of the increased levels of p21 and p27 observed in the $Id2^{-/-}$ embryos [52], which in the $Rb^{-/-}$ embryos may be sufficient to prevent hyperproliferation and at the same time allow the bHLH transcription factors to induce differentiation. Because Id2 is not expressed in muscle [50••], the lack of Id2 is not able to restore differentiation in this tissue. Therefore, in contrast to the suggestion that Id2 and pRB work in a linear pathway [50••], Id2 and pRB may work in two parallel pathways controlling proliferation, differentiation and apoptosis. If this is correct, it may suggest that the deletion of one of the other Id family members (which do not bind to pRB) may restore muscle differentiation in pRb-deficient mouse embryos.

Conclusions and perspectives

In the past few years, mouse genetic models have extended our knowledge about the genetic requirements for the induction of apoptosis regulated by pRB and p53. Moreover, gene-expression profiling has identified a number of target genes that can explain how these two tumour suppressors regulate apoptosis.

The rate of identification of novel p53 target genes is currently accelerating, and we expect to see this trend continue over the coming years. One of the biggest challenges currently facing p53 research is to collate all of the data into a working model of p53 in tumorigenesis. To date, the significance of p53 phosphorylation sites, for example, has been difficult to assess because of discrepancies between data obtained in different tumour cell lines from different genetic backgrounds. It is now clear that p53 cannot merely be considered as 'active' or 'inactive', but is very much subject to modulation by tissue-specific and stimulus-specific factors. The use of mouse 'knock-in' models to investigate the function of p53 mutants *in vivo* should shed some light on this issue. The long-term goal will be to correlate these data with the observed behaviour of p53 and its regulators and target genes in human tumours.

It is now evident that loss of pRB loss results in apoptosis in normal cells, and that any mechanism suppressing apoptosis would provide an opportunity for pRB-deficient cells to survive. In this perspective it becomes clear why there is a selective pressure to inactivate genes that mediate apoptosis. This also explains why roughly 50% of all tumour cells do not express functional p53. Although *ARF* is mutated in a substantial number of human tumours, it is at present unclear whether deletion of *ARF* suppresses apoptosis *in vivo*. Therefore, we are unable to account for the genetic alterations that allow cell survival in a relatively high fraction of human cancers. These alterations might include an increased expression of survival signals (e.g. in the form of growth factors), or genetic alterations in genes that are activated by p53 or E2F, or in components that are central to the execution of apoptosis.

Recently, this concept has been confirmed further by the demonstration that *APAF1* expression is lost in malignant melanomas through a combination of allelic loss and hypermethylation of the *APAF1* gene [23••]. Moreover, Caspase 8 — a gene that is involved in both drug- and death-receptor-induced apoptosis — has been frequently found to be deleted or silenced through hypermethylation in childhood neuroblastoma [53••]. In addition to providing further incentive to uncover the molecular mechanisms that regulate p53- and E2F-induced apoptosis, these results suggest a possible therapeutic approach to induce apoptosis in metastatic melanomas and neuroblastomas by using, for example, inhibitors of DNA methylation such as 5-aza-2′-deoxycytidine.

Acknowledgements

We thank Claire Attwooll and Mark Pearson for helpful comments on the manuscript. Work in the authors' laboratory is supported by grants from the Italian Association for Cancer Research (AIRC), the Italian Foundation for Cancer Research (FIRC), the Human Science Frontiers Science Programme, the EU's Fifth Framework Program and the Association for International Cancer Research.

References and recommended reading

Papers of particular interest, published within the annual period of review, have been highlighted as:

- • of special interest
- •• of outstanding interest

1. Donehower L, Harvey M, Slagle B, McArthur M, Montgomery C, Butel J, Bradley A: **Mice deficient for p53 are developmentally normal but susceptible to spontaneous tumours.** *Nature* 1992, 356:215-221.

2. Jacks T, Remington L, Williams BO, Schmitt EM, Halachmi S, Bronson RT, Weinberg RA: **Tumor spectrum analysis in p53-mutant mice.** *Curr Biol* 1994, 4:1-7.

3. Levine AJ: **p53, the cellular gatekeeper for growth and division.** *Cell* 1997, 88:323-331.

4. Giaccia AJ, Kastan MB: **The complexity of p53 modulation: emerging patterns from divergent signals.** *Genes Dev* 1998, 12:2973-2983.

5. Lakin ND, Jackson SP: **Regulation of p53 in response to DNA damage.** *Oncogene* 1999, 18:7644-7655.

6. Banin S, Moyal L, Khostravi R, Shieh SY, Taya Y, Anderson CW, Chessa L, Smorodinsky NI, Prives C, Shiloh Y, Ziv Y: **Enhanced phosphorylation of p53 by ATM in response to DNA damage.** *Science* 1998, 281:1674-1677.

7. Canman CE, Lim DS, Cimprich KA, Taya Y, Tamai K, Sakaguchi K, Appella E, Kastan MB, Siliciano DD: **Activation of the ATM kinase by ionising radiation and phosphorylation of p53.** *Science* 1998, 281:1677-1679.

8. Chehab NH, Malikzay A, Appel M, Halazonetis TD: **Chk2/hCds1 functions as a DNA damage checkpoint in G_1 by stabilizing p53.** *Genes Dev* 2000, 14:278-288.

9. • Chao C, Saito S, Kang J, Anderson CW, Appella E, Xu Y: **p53 transcriptional activity is essential for p53-dependent apoptosis following DNA damage.** *EMBO J* 2000, 19:4967-4975.

These two papers [9•,10•] describe the use of a mouse knock-in system to analyse the apoptotic activity of a transcriptionally inactive p53 mutant *in vivo*. Both groups show that this mutant cannot induce apoptosis and consequently does not suppress transformation.

10. • Jimenez GS, Nister M, Stommel JM, Beeche M, Barcarse EA, Zhang XQ, O'Gorman S, Wahl GM: **A transactivation-deficient mouse model provides insights into Trp53 regulation and function.** *Nat Genet* 2000, 26:37-43.

See annotation [9•].

11. Miyashita T, Krajewski S, Krajewska M, Wang HG, Lin HK, Liebermann DA, Hoffman B, Reed JC: **Tumor suppressor p53 is a regulator of *bcl-2* and *bax* gene expression *in vitro* and *in vivo*.** *Oncogene* 1994, 9:1799-1805.

12. Miyashita T, Reed JC: **Tumor suppressor p53 is a direct transcriptional activator of the human *bax* gene.** *Cell* 1995, 80:293-299.

13. Owen-Schaub LB, Zhang W, Cusack JC, Angelo LS, Santee SM, Fujiwara T, Roth JA, Deisseroth AB, Zhang WW, Kruzel E, Radinsky R: **Wild-type human p53 and a temperature-sensitive mutant induce Fas/APO-1 expression.** *Mol Cell Biol* 1995, 15:3032-3040.

14. Polyak K, Xia Y, Zweier JL, Kinzler KW, Vogelstein B: **A model for p53-induced apoptosis.** *Nature* 1997, 389:300-305.

15. • Nakano K, Vousden K: **PUMA, a novel proapoptotic gene, is induced by p53.** *Mol Cell* 2001, 7:683-694.

The first of nine recent articles [15•–20•,22•,24•,26•] that describe the identification of novel p53 target genes that are involved in apoptosis. These genes have all been identified by expression analysis and each of them has been shown to be required for efficient induction of apoptosis following p53 activation in tissue culture cells.

16. • Yu J, Zhang L, Hwang PM, Kinzler KW, Vogelstein B: **PUMA induces the rapid apoptosis of colorectal cancer cells.** *Mol Cell* 2001, 7:673-682.

See annotation [15•].

17. • Oda E, Ohki R, Murasawa H, Nemoto J, Shibue T, Yamashita T, Tokino T, Taniguchi T, Tanaka N: **Noxa, a BH3-only member of the Bcl-2 family and candidate mediator of p53-induced apoptosis.** *Science* 2000, 288:1053-1058.

See annotation [15•].

18. • Ryan KM, Ernst MK, Rice NR, Vousden KH: **Role of NF-κB in p53 mediated programmed cell death.** *Nature* 2000, 404:892-897.

See annotation [15•].

19. • Oda K, Arakawa H, Tanaka T, Matsuda K, Tanikawa C, Mori T, Nishimori H, Tamai K, Tokino T, Nakamura Y, Taya Y: **p53AIP1, a potential mediator of p53-dependent apoptosis, and its regulation by Ser-46-phosphorylated p53.** *Cell* 2000, 102:849-862.

See annotation [15•].

20. • Lin Y, Ma W, Benchimol S: **Pidd, a new death-domain-containing protein, is induced by p53 and promotes apoptosis.** *Nat Genet* 2000, 26:122-127.

See annotation [15•].

21. Hengartner MO: **The biochemistry of apoptosis.** *Nature* 2000, 407:770-776.

22. • Moroni MC, Hickman ES, Caprara G, Denchi E, Colli E, Cecconi F, Müller H, Helin K: ***APAF1* is a transcriptional target for E2F and p53.** *Nat Cell Biol* 2001, 3:552-558.

See also annotation [15•]. In addition to identifying *APAF1* as a p53-regulated gene, this paper also demonstrates that *APAF1* is a direct target for pRB/E2F regulation, and that *APAF1* is a mediator of E2F-induced apoptosis.

23. •• Soengas MS, Capodieci P, Polsky D, Mora J, Esteller M, Opitz-Araya X, McCombie R, Herman JG, Gerald WL, Lazebnik YA *et al.*: **Inactivation of the apoptosis effector Apaf-1 in malignant melanoma.** *Nature* 2001, 409:207-211.

An exceptional paper that identifies the *APAF1* gene as a target for promoter hypermethylation in melanoma. This not only shows that *APAF1* is a tumour suppressor gene but also raises the possibility that other p53-induced genes may be targeted in tumorigenesis.

24. • Okamura S, Arakawa H, Tanaka T, Nakanishi H, Ng CC, Taya Y, Monden M, Nakamura Y: **p53DINP1, a p53-inducible gene, regulates p53-dependent apoptosis.** *Mol Cell* 2001, 8:85-94.

See annotation [15•].

25. • Ashcroft M, Taya Y, Vousden KH: **Stress signals utilize multiple pathways to stabilize p53.** *Mol Cell Biol* 2000, 20:3224-3233.

An interesting paper showing that p53-induced gene expression may be specific to the type of stress stimulus applied.

26. • Attardi LD, Reczek EE, Cosmas C, Demicco EG, McCurrach ME, Lowe SW, Jacks T: **PERP, an apoptosis-associated target of p53, is a novel member of the PMP-22/gas3 family.** *Genes Dev* 2000, 14:704-718.

See annotation [15•].

27. Relaix F, Wei XJ, Li W, Pan J, Lin Y, Bowtell DD, Sassoon DA, Wu X: **Pw1/Peg3 is a potential cell death mediator and cooperates with Siah1a in p53-mediated apoptosis.** *Proc Natl Acad Sci USA* 2000, 97:2105-2110.

28. Weinberg RA: **The retinoblastoma protein and cell cycle control.** *Cell* 1995, 81:323-330.

29. Lipinski MM, Jacks T: **The retinoblastoma gene family in differentiation and development.** *Oncogene* 1999, 18:7873-7882.

30. Hanahan D, Weinberg RA: **The hallmarks of cancer.** *Cell* 2000, 100:57-70.

31. Gallie BL, Campbell C, Devlin H, Duckett A, Squire JA: **Developmental basis of retinal-specific induction of cancer by RB mutation.** *Cancer Res* 1999, 59:1731s-1735s.

32. Jiang Z, Guo Z, Saad FA, Ellis J, Zacksenhaus E: **Retinoblastoma gene promoter directs transgene expression exclusively to the nervous system.** *J Biol Chem* 2001, 276:593-600.

33. • Lipinski MM, Macleod K, Williams BO, Mullaney TL, Crowley D, Jacks T: **Cell-autonomous and non-cell autonomous functions of the Rb tumor suppressor in developing central nervous system.** *EMBO J* 2001, 20:3402-3413.

By generating chimaeric mice composed of wild-type and Rb-deficient cells, the authors show that pRB has a non-cell-autonomous (in differentiation and apoptosis) and a cell-autonomous (in cell-cycle control) role during development.

34. Morgenbesser SD, Williams BO, Jacks T, DePinho RA: **p53-dependent apoptosis produced by pRb-deficiency in the developing mouse lens.** *Nature* 1994, 371:72-74.

35. Macleod KF, Hu Y, Jacks T: **Loss of Rb activates both p53-dependent and independent cell death pathways in the developing mouse nervous system.** *EMBO J* 1996, 15:6178-6188.

36. Dyson N: **The regulation of E2F by pRB-family proteins.** *Genes Dev* 1998, 12:2245-2262.

37. Helin K: **Regulation of cell proliferation by the E2F transcription factors.** *Curr Opin Genet Dev* 1998, **8**:28-35.

38. Vigo E, Müller H, Prosperini E, Hateboer G, Cartwright P, Moroni MC, Helin K: **CDC25A phosphatase is a target of E2F and is required for efficient E2F-1 induced S phase.** *Mol Cell Biol* 1999, **19**:6379-6395.

39. Tsai KY, Hu Y, Macleod KF, Crowley D, Yamasaki L, Jacks T: **Mutation of E2F1 supresses apoptosis and inappropriate S-phase entry and extends survival of Rb-deficient mouse embryos.** *Mol Cell* 1998, 2:293-304.

40. • Ziebold U, Reza T, Caron A, Lees J: **E2F3 contributes both to the inappropriate proliferation and to the apoptosis arising in *Rb* mutant embryos.** *Genes Dev* 2001, **15**:386-391.
By analysing mice lacking *E2F3* and *Rb*, the authors show that E2F3 significantly contributes to apoptosis and inappropriate cell proliferation resulting from pRB loss *in vivo*.

41. DeGregori J, Leone G, Miron A, Jakoi L, Nevins JR: **Distinct roles for E2F proteins in cell growth control an apoptosis.** *Proc Natl Acad Sci USA* 1997, **94**:7245-7250.

42. Bates S, Phillips AC, Clark PA, Stott F, Peters G, Ludwig RL, Vousden KH: **$p14^{ARF}$ links the tumour suppressors RB and p53.** *Nature* 1998, **395**:124-125.

43. Sherr CJ: **Tumor surveillance via ARF–p53 pathway.** *Genes Dev* 1998, **12**:2984-2991.

44. Zindy F, Eischen CM, Randle DH, Kamijo T, Cleveland JL, Sherr CJ, Roussel MF: **Myc signaling via the ARF tumor suppressor regulates p53-dependent apoptosis and immortalization.** *Genes Dev* 1998, **12**:2424-2433.

45. • Irwin M, MC MCM, Phillips AC, Seelan RS, Smith DI, Liu W, Flores ER, Tsai KY, Jacks T, Vousden KH, Kaelin Jr WG: **Role for the p53 homologue p73 in E2F-1-induced apoptosis.** *Nature* 2000, **407**:645-648.
An interesting paper that, together with [46•], identifies p73 as a target gene for E2F1. Analysis of p73-deficient fibroblasts and the expression of dominant-negative versions of p73 suggest that p73 has a role in E2F1-induced apoptosis.

46. • Stiewe T, Putzer BM: **Role of the p53-homologue p73 in E2F1 induced apoptosis.** *Nat Genet* 2000, **26**:464-469.
See annotation [45•].

47. • Müller H, Bracken AP, Vernell R, Moroni MC, Christians F, Grassilli E, Prosperini E, Vigo E, Oliner JD, Helin K: **E2Fs regulate the expression of genes involved in differentiation, development, proliferation and apoptosis.** *Genes Dev* 2001, **15**:267-285.
High-density oligonucleotide array analysis is used to identify genes whose expression pattern changed in response to activation of E2F1, E2F2 and E2F3. More than 1000 genes are identified whose expression changes significantly within 8 hours of increased levels of E2F activity. Several of the E2F-regulated genes identified are essential for a number of cellular processes, such as differentiation and apoptosis.

48. Soengas MS, Alarcón RM, Yoshida H, Giaccia AJ, Hakem R, Mak TW, Lowe SW: **Apaf-1 and Caspase-9 in p53-dependent apoptosis and tumor inhibition.** *Science* 1999, **284**:156-159.

49. Phillips AC, Ernst MK, Bates S, Rice NR, Vousden KH: **E2F-1 potentiates cell death by blocking antiapoptotic signaling pathways.** *Mol Cell* 1999, 4:771-781.

50. •• Lasorella A, Noseda M, Beyna M, Yokota Y, Iavarone A: **Id2 is a retinoblastoma protein target and mediates signalling by Myc oncoproteins.** *Nature* 2000, **407**:592-598.
A very interesting paper showing that inactivation of *Id2* rescues embryonic lethality of Rb-deficient embryos. Furthermore, *Id2* is identified as a target gene for N-Myc in neuroblastoma. A model is suggested in which Id2 is a target for pRB regulation in normal cells, but Id2 inactivates pRB in neuroblastomas.

51. Yokota Y, Mansouri A, Mori S, Sugawara S, Adachi S, Nishikawa SI, Gruss P: **Development of peripheral lymphoid organs and natural killer cells depends on the helix–loop–helix inhibitor Id2.** *Nature* 1999, **397**:702-706.

52. Mori S, Nishikawa SI, Yokota Y: **Lactation defect in mice lacking the helix–loop–helix inhibitor Id2.** *EMBO J* 2000, **19**:5772-5781.

53. •• Teitz T, Wie T, Valentine MB, Vanin EF, Grenet J, Valentine VA, Behm FG, Look AT, Lahti JM, Kidd VJ: **Caspase 8 is deleted or silenced preferentially in childhood neuroblastomas with amplification of *MYCN*.** *Nat Med* 2000, **6**:529-535.
The study demonstrates that the gene for Caspase 8 is frequently inactivated in neuroblastomas with amplification of the *MYCN* oncogene, suggesting that Caspase 8 acts as a tumour suppressor.

54. Wu GS, Burns TF, McDonald ER, Jiang W, Meng R, Krantz ID, Kao G, Gan DD, Zhou JY, Muschel R *et al.*: **KILLER/DR5 is a DNA damage-inducible p53-regulated death receptor gene.** *Nat Genet* 1997, **17**:141-143.

Proc. Natl. Acad. Sci. USA
Vol. 96, pp. 7992–7997, July 1999
Developmental Biology

DIO-1 is a gene involved in onset of apoptosis *in vitro*, whose misexpression disrupts limb development

(transcription factors/interdigital webs)

DAVID GARCÍA-DOMINGO*, ESTHER LEONARDO*, ALF GRANDIEN*†, PEDRO MARTÍNEZ*, JUAN PABLO ALBAR*, JUAN CARLOS IZPISÚA-BELMONTE‡, AND CARLOS MARTÍNEZ-A*§

*Department of Immunology and Oncology, Centro Nacional de Biotecnología, Universidad Autónoma, Campus de Cantoblanco, E-28049 Madrid, Spain; †Department of Immunology, Stockholm University, Stockholm, Sweden; and ‡The Salk Institute, 10010 North Torrey Pines Road, La Jolla, CA 92037

Communicated by A. Garcia-Bellido, Autonomous University of Madrid, Madrid, Spain, April 23, 1999 (received for review March 3, 1999)

ABSTRACT **The *DIO-1* (*death inducer-obliterator-1*) gene, identified by differential display PCR in pre-B WOL-1 cells undergoing apoptosis, encodes a putative transcription factor whose protein has two Zn finger motifs, nuclear localization signals, and transcriptional activation domains, expressed in the limb interdigitating webs during development. When overexpressed, *DIO-1* translocates to the nucleus and activates apoptosis *in vitro*. Nuclear translocation as well as induction of apoptosis are lost after deletion of the nuclear localization sequences. *DIO-1* apoptotic induction is prevented by caspase inhibitors and Bcl-2 overexpression. The *in vivo* role of *DIO-1* was studied by misexpressing *DIO-1* during chicken limb development. The most frequently observed phenotype was an arrest in limb outgrowth, an effect that correlates with the inhibition of mesodermal and ectodermal genes involved in this process. Our data demonstrate the ability of *DIO-1* to trigger apoptotic processes *in vitro* and suggest a role for this gene in cell death during development.**

Apoptosis is a major form of cell death, characterized morphologically by chromatin condensation, nuclear disruption, and formation of cytosol containing apoptotic bodies. It is an efficient mechanism for eliminating unwanted cells and is of central importance for development and homeostasis in metazoan animals (1). Many different signals within or from outside the cell have been shown to influence the decision between life and death (2). Most are controlled through triggering of specific receptors, which leads to activation of specific mediators; they may then act to suppress or promote activation of the death program. It is hence not surprising that initiation of apoptosis is precisely regulated.

A common meeting point for cell death signals is the cytoplasm, where the caspases exert their function and are blocked by their inhibitors (3–6). Very little is known as to how these signals are transmitted to the nucleus. A caspase-activated DNase (CAD) and its inhibitor (ICAD) have recently been identified in the cytoplasmic fraction of a mouse lymphoma cell line. Caspase pathway activation by different stimuli cleaves ICAD, allowing CAD to enter the nucleus and degrade chromosomal DNA (7, 8). In addition to the caspases, inducible gene products also appear to be required for apoptotic death in some cell types (9). Evidence for this was derived from experiments in which cell death could be suppressed by the inhibition of RNA or protein synthesis in cells that should otherwise die (10), suggesting that gene transcription and RNA translation are required for death to occur in these cells. Indeed, transcriptional activation of specific genes is absolutely required for physiological apoptosis in both insect and vertebrate embryos (10, 11). Several transcriptional regulators are known to control apoptosis, among which p53 (12), Nur77 (13), the glucocorticoid receptor (14), STAT1 (15), c-myc (12, 16), c-jun (17), and NF-κB (18) have been identified to date.

Much of the natural cell death that occurs during insect and vertebrate development appears to be mediated by the transcriptional activation of killer genes. Although no such genes have yet been identified in vertebrates, recent studies in the fly *Drosophila melanogaster* have uncovered three components of the genetic program controlling programmed cell death (PCD), *hid*, *grim*, and *reaper*, whose transcriptional activation precedes, induces, and is necessary for PCD by apoptosis (19–21). The three genes map to a single genetic complex and function as death switches that are regulated at the level of transcription. Their ectopic activation triggers apoptosis in otherwise viable cells, and their inactivation prevents apoptosis of cells that would normally undergo PCD. We and others have recently demonstrated that the expression of one of these genes, *grim*, activates apoptosis in mammalian cells, implying conservation during metazoan evolution of both the gene and the mechanisms required to trigger cell death (9).

The developing limb is perhaps one of the best-suited model systems for the study of this process, because fine tuning is required between cell proliferation and cell apoptosis to allow proper limb modeling, a process subject to intervention without endangering embryo viability. Whilst much has recently been learned regarding factors involved in cell proliferation, less is known about the mechanisms implicated in programmed cell death during development. It has recently been shown that inhibition of NF-κB translocation by viral overexpression of a transdominant-negative IκB leads to perturbation of limb outgrowth (22). We have now tested *in vivo* the effect of a, to our knowledge, novel gene, *DIO-1* (*death inducer-obliterator-1*), identified by differential display PCR in pre-B cells undergoing apoptosis. Its mRNA and protein are present at very low levels in the cytoplasm. Once an appropriate apoptotic signal is detected, the protein translocates to the nucleus and up-regulation is observed at both transcript and protein levels. When overexpressed, it induces apoptosis in cell lines growing *in vitro*, which is prevented by blocking caspase activity. The protein encoded, DIO-1, is expressed in the limb interdigitating membranes during development. *DIO-1* expression in distal proliferating mesodermal cells of the developing chicken limb bud prevents limb outgrowth, an effect that correlates with inhibition of mesodermal and ectodermal genes involved in limb outgrowth. These data demonstrate the ability of *DIO-1* to trigger apoptotic processes *in vitro*, as well as the

The publication costs of this article were defrayed in part by page charge payment. This article must therefore be hereby marked "*advertisement*" in accordance with 18 U.S.C. §1734 solely to indicate this fact.

PNAS is available online at www.pnas.org.

Abbreviations: AER, apical ectodermal ridge; E2, 17β-estradiol; NLS, nuclear localization signal.

Data deposition: The sequence reported in this paper has been deposited in the GenBank database (accession no. AJ238332).

§To whom reprint requests should be addressed. e-mail cmartineza@cnb.uam.es.

utility of limb development as a model system to characterize genes involved in apoptosis.

MATERIALS AND METHODS

Cloning of *DIO-1*. Differential display experiments were performed by using an RNAmap kit (GenHunter, Brookline, MA) according to the manufacturer's specifications. Briefly, 200 ng of total cytoplasmic RNA (after DNase treatment with the MessageClean Kit; GenHunter) isolated from WOL-1 cells at 0, 2, 4, and 8 h after IL-7 withdrawal were reverse transcribed with oligo(dT) primers ($T_{12}MN$) in the presence of Moloney murine leukemia virus reverse transcriptase. They were amplified with several combinations of 5′ decamer arbitrary primers and the $T_{12}MN$ used for reverse transcription in the presence of [^{35}S]dATP (1,200 Ci/mmol). Amplified products were resolved in an 8-M urea/6% polyacrylamide DNA sequencing gel and analyzed by autoradiography. Bands of interest were isolated, reamplified, cloned in the pCR-Script SK(+) vector (Stratagene), and used for Northern analysis and sequencing. *DIO-1* cDNA was obtained from WOL-1 cDNA by 5′ rapid amplification of cDNA ends (RACE) by using a Marathon cDNA Amplification Kit (CLONTECH), with the 3′ primer L282 (5′-AGGTGTACCTTGTACAGCAGTGAAAC-3′). The resulting 2.6-kbp band was excised from the gel and cloned in the TA-type vector pGEM-T (Promega). Resulting clones were sequence analyzed for orientation, and the oriented sense with respect to the T7 promoter was called DIO-1pGEM-T. To confirm the ORF sequence obtained, a cDNA library from mouse brain cloned in λZAP II (Stratagene) was screened by probing with the RACE clone; the same probe was used to screen a human fetal kidney cDNA library (CLONTECH) from which the human *DIO-1* homologue was cloned.

Cells and Transfections. WOL-1 cells were derived from adult BALB/c mouse bone marrow. WOL-1 is an untransformed IL-7-dependent stroma cell- independent pre-BI cell line, capable of reconstituting irradiated severe combined immunodeficient mice. Cells were cultured in Iscove's modified Dulbecco's medium supplemented with penicillin (100 units/ml)/streptomycin (100 μg/ml)/1 mM sodium pyruvate/nonessential amino acids/50 μM 2-mercaptoethanol/2 mM L-glutamine/10% FCS/IL-7 (3% supernatant from a murine IL-7-producing cell line). The Ba/F3 and FL5.12 cell lines were maintained in RPMI medium 1640 with 10% FCS and 5% supernatant of a murine IL-3-producing cell line, whereas A20 and WEHI-231 grew in the same medium without IL-3. The FL5.12hBcl-2 stable cell line was cultured in 1 mg/ml G-418 (Calbiochem). MEF(10.1)Val5MycER cells were cultured at 39°C in phenol red-free DMEM containing 10% FCS. Where indicated, 1 μM 17β-estradiol (E2) was added to activate the MycER fusion protein after 24 h FCS starvation (12). WOL-1, A20, Ba/F3, and FL5.12 cell lines were cultured at 37°C, and all cell lines were maintained in a humidified atmosphere with 5% CO_2.

Transient DNA transfection was performed by electroporation. For each transfection, 2×10^6 log phase cells were collected by centrifugation and resuspended in 200 μl of RPMI medium 1640 without FCS. After addition of 10 μg of plasmid DNA (1 mg/ml), samples were gently shaken and electroporated in a 0.4-cm electrode gap gene pulser cuvette at 960 μF and 320 V with a GenePulser (Bio-Rad). Samples were diluted with 6 ml of the same medium supplemented with 10% FCS and incubated at 37°C in a humidified atmosphere with 5% CO_2. Cells were analyzed for cell-cycle staining by FACS at 48 h after electroporation.

Northern Blot Analysis. Total cytoplasmic RNA was prepared as described (23). RNA (10 μg) was Northern blotted by using a ^{32}P-labeled *DIO-1* riboprobe made by DIO-1pGEM-T digestion with *Bgl*II and *in vitro* transcribed from SP6 by using the Riboprobe *In Vitro* Transcription System (Promega). Hybridization was performed in 50% formamide at 65°C; washes were in 0.1× SSC + 0.1% SDS at 80°C. Blots were exposed on Kodak X-Omat AR film at −70°C with two intensifying screens.

Antibody Production and Western Blot. We synthesized a peptide corresponding to amino acids 58–72 of murine *DIO-1* with an additional N-terminal cysteine (CSLRRSGRQPKRTERV); it was coupled to maleimide-activated keyhole limpet hemocyanin and the purified conjugate injected into New Zealand White rabbits. Polyclonal antibody was affinity purified on a peptide-thiopropyl Sepharose column. For Western blot, cells were collected at different times after IL-7 removal from culture medium; 5×10^5 cells were lysed with RIPA buffer (0.15 mM NaCl/0.05 mM Tris·HCl, pH 7.2/1% Triton X-100/1% sodium deoxycholate/0.1% SDS), and the total extract separated in 8% SDS/PAGE, transferred and incubated with the affinity-purified polyclonal anti-*DIO-1* antibody (1:100 dilution in TBS-1% nonfat dry milk). Protein-loading equivalence was confirmed by Ponceau S staining.

***In Situ* Hybridization and Histology.** Whole-mount *in situ* hybridization was as described (24) with minor modifications (25). The *DIO-1* digoxigenin probe was made by *Bgl*II digestion of the DIO-1pGEM-T and transcription from the SP6 promoter. The probe used for *Lhx-2* (700 bp) encompasses the homeobox and the second LIM (*lin-11, Isl-1, mec-3*) domain. The remaining probes have been described elsewhere and include *Msx-1* (26), *Fgf-8* (27), and *NF-κB* (22). To visualize cartilage, embryos were fixed in trichloroacetic acid after viral infection, stained with 0.1% alcian green, and dehydrated/cleared in methyl salicylate.

Virus Production and Injection Protocols. Chicken embryos (from MacIntyre Poultry, San Diego, CA, or SPAFAS, Preston, CT) were infected with a virus containing the *DIO-1* ORF. Virus preparation and injections were as previously described (28). After injection, embryos were incubated at 37°C and fixed at different time points for *in situ* hybridization or phenotypic analysis.

RESULTS

Isolation of *DIO-1* cDNA: Protein Structure and Sequence Relationships. To search for genes implicated in apoptosis, we used the differential display PCR (DDRT-PCR) technique (29) using mRNA obtained from the WOL-1 pre-B cell line as a target. WOL-1 was derived from BALB/c adult bone marrow; it grows exponentially in the presence of IL-7 and undergoes apoptosis on IL-7 withdrawal. The DDRT-PCR technique gave rise to several positive bands, 10 of which were initially identified as undergoing up- or down-regulation during apoptotic death and were therefore considered candidates for subsequent analysis. They were further amplified, sequenced, and compared with known gene sequences by using the National Center for Biotechnology Information BLAST program (30). Of these, one band (DIO-1) revealed that the nucleotide sequence was a gene that showed no significant identity to any known gene or translated products in the databases. To confirm the sequence obtained by rapid amplification of cDNA ends (RACE), a murine cDNA library was screened by using a labeled *DIO-1* probe. Five positive clones were identified and characterized by restriction mapping and sequencing. Analysis of the cDNA revealed inserts identical in sequence to the ORF cloned by RACE. The longest ORF corresponds to a 614-aa protein (Fig. 1*A*) and shows a Kozak consensus sequence before the ATG (considered as the +1 position) known to be crucial for initiation of translation (31). It also comprises a putative nuclear localization signal (NLS) and transcriptional activation domain in the N-terminal region, two central Zn finger motifs, and a lysine-rich carboxyl terminus. Having analyzed the domains of the putative pro-

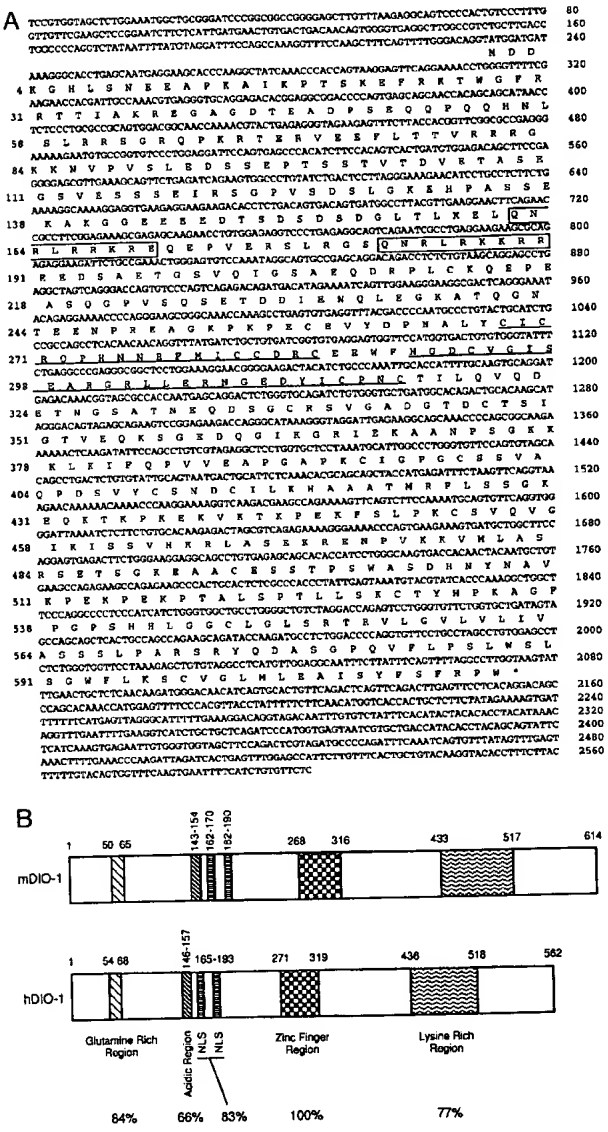

FIG. 1. Nucleotide and predicted amino acid sequences of murine and human *DIO-1*. (*A*) The bipartite NLS sequence is boxed, and the zinc finger motifs are underlined. (*B*) Schematic representation of the predicted ORF of murine and human *DIO-1*. The start and end positions of the amino acids defining the motifs are numbered above. Percentages indicate degree of identity between human and mouse for each domain. Overall similarity is 74%.

tein, we sought to determine their degree of conservation in closely related species to assess their function. A human cDNA library was screened by using the murine clone as probe; positive clones were sequenced and showed strong similarity to the murine gene in the ORF, with a high degree of structural and compositional conservation (Fig. 1*B*).

***DIO-1* Is Present in All Tissues and Its Levels Are Up-Regulated During Apoptosis.** To study *DIO-1* gene regulation during apoptosis, *DIO-1* expression pattern was examined by Northern blot analysis. Various tissues were analyzed to determine *DIO-1* transcript distribution, and two 9.5- and 5.4-Kb mRNA species were detected in all tissues tested (Fig. 2*A*). Southern blot analysis of genomic DNA showed that *DIO-1* is a single-copy gene in both mouse and human. RNA samples were isolated from several cell lines in exponential growth or undergoing apoptosis as a result of various experimental treatments. In the exponential growth phase, WOL-1 cells express low levels of *DIO-1* mRNA, which increase after induction of apoptosis (Fig. 2*B*). *DIO-1* is up-regulated in IL-7-deprived cells or those treated with IFN-γ or dexamethasone, but not in cells treated with etoposide, UV irradiation, or in those undergoing p53-induced cell death (Fig. 2*B*). It is also up-regulated in anti-IgM-treated WEHI-231 cells. In MEF(10.1)Val5MycER cells, up-regulation is observed in the absence of serum after addition of E2, but not before or at 32°C (even in the presence of E2 or serum). Up-regulation of *DIO-1* mRNA levels in cells undergoing apoptosis was confirmed in Western blot by using a polyclonal anti-*DIO-1* antibody raised against a synthetic peptide comprising amino acids 58–72. In cell extracts derived from WOL-1 cells undergoing IL-7 deprivation-induced apoptosis, a 67-kDa band was up-regulated 2 hr after induction (Fig. 2*C*), but not after etoposide-induced cell death (data not shown). In all cases in which up-regulation of the *DIO-1* transcript or of the DIO-1 protein itself was detected, there was a clear peak in the kinetic levels of *DIO-1* up-regulation before any signs of cell death were detectable.

***DIO-1*-Induced Apoptosis Is Inhibited by Bcl-2 and Z-VAD and Lost by Deletion of the NLS.** The role of *DIO-1* in the apoptotic process was evaluated by transient transfection of the gene into several cell lines and examination of cell death kinetics. Transfection of a *DIO-1* expression plasmid into Ba/F3 cells results in a dramatic loss of cell viability at 48 hr after transfection (Fig. 3). All cells displayed morphological alterations characteristic of apoptosis, becoming rounded, condensed, and finally dying. This effect was specific in that transfection of Ba/F3 with an empty vector had no effect on cell survival. To verify the generality of this observation, *DIO-1* constructs were transfected into A20 or FL5.12 cells (Fig. 3). In both cases, apoptosis was induced after kinetics similar to those observed for Ba/F3. Transfection into MEF(10.1)Val5MycER cells gave rise to apoptotic morphology as assessed by 4′6′-diamidino-2-phenylindole staining; using the *DIO-1*-specific antibody, we found that endogenous *DIO-1* is located in the cytoplasm of MEF(10.1)Val5MycER cells in exponential growth. When apoptosis is triggered in these cells by addition of E2 at 39°C in the absence of serum, *DIO-1* is translocated to the nucleus (not shown). This translocation appears to be critical for activation of the apoptotic pathway, as deletion of the NLS renders the DIO-1 protein unable to translocate to the nucleus, thus impairing its ability to trigger apoptosis (Fig. 3). When *DIO-1* was transfected into stable FL5.12 cells overexpressing human Bcl-2, cells were resistant to apoptosis, showing that Bcl-2 coexpression inhibits *DIO-1* death-promoting activity, as has also been described for other systems (32). We also incubated *DIO-1*-transfected FL5.12 cells alone or in the presence of the caspase inhibitor Z-VAD-fmk. After 48-h expression in the presence of IL-3, the apoptosis induced by *DIO-1* was completely blocked because of caspase inhibition, an observation that again clearly suggests that the death pathway induced by this gene requires caspase activity. Finally, extensive efforts to derive stable *DIO-1* transfectants in these three cell lines were unsuccessful, suggesting the lethality of *DIO-1* expression in these cells. All together, these results show that *DIO-1* overexpression results in the activation of a cell death program analogous to that operative in other systems, and that activation of the death pathway requires *DIO-1* translocation to the nucleus, where it probably performs a function compatible with its structure as a transcription factor.

Alteration of Limb Development by *DIO-1* Overexpression. Using whole-mount *in situ* hybridization, we also studied *DIO-1* expression throughout mouse development, which is expressed in the most distal limb cells on developmental day 10.5 (Fig. 4) and close to or within the limb interdigitating webs on day 12.5 (Fig. 4 *Inset*). Based on the *in vitro* effects and *in vivo* expression pattern described above, as well as on the presence of *DIO-1* transcripts in the limb cells undergoing

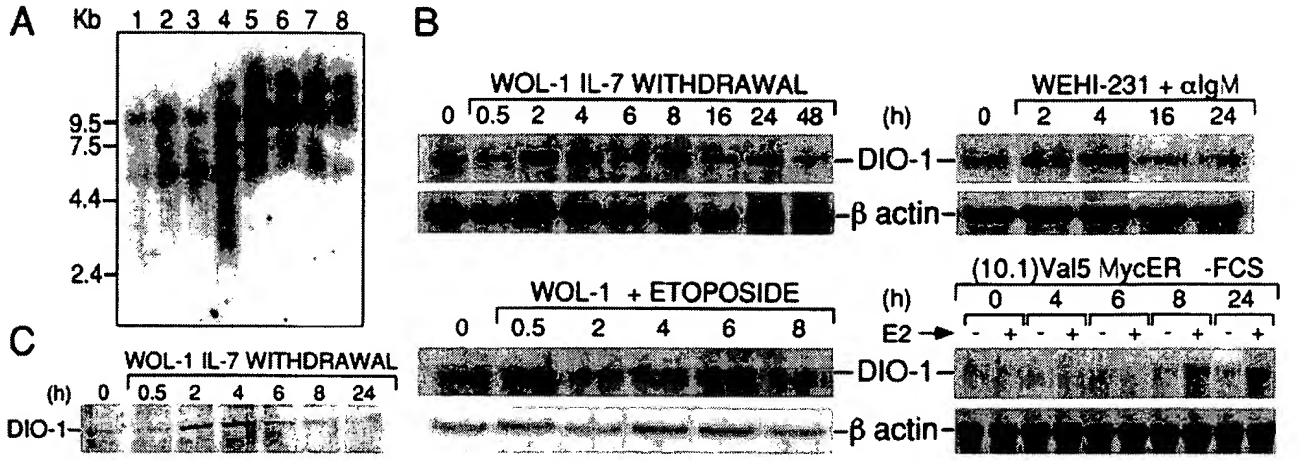

FIG. 2. *DIO-1* is differentially expressed under several apoptotic conditions and induces apoptosis when overexpressed. (*A*) *DIO-1* expression was analyzed in murine tissues by hybridization with the *DIO-1* riboprobe of a mouse MTN blot (CLONTECH). Molecular size markers are indicated on the left. Lanes: 1, heart; 2, brain; 3, spleen; 4, lung; 5, liver; 6, skeletal muscle; 7, kidney; 8, testis. (*B*) Northern blots containing 10 μg per lane of total cytoplasmic RNA from the indicated cell lines, treated with several apoptotic stimuli at different time points, were hybridized to the *DIO-1* riboprobe. The blots were reprobed with an actin probe for normalization of the amounts loaded. (*C*) Western blot analysis of WOL-1 cells driven to apoptosis by IL-7 starvation. The position of the *DIO-1* gene product is indicated.

apoptotic cell death, we hypothesized that *DIO-1* may influence the control of cell proliferation and death during vertebrate limb development (see ref. 33 for a review on vertebrate limb outgrowth).

Retroviral technology was used to misexpress *DIO-1* in the chicken limb. A replication-competent retroviral vector containing the *DIO-1* ORF was injected into limb primordia at stages 10–23. The consequences of *DIO-1* expression were analyzed in embryo limb buds throughout development. At 60–72 h after injection, infected limb buds failed to develop a normal apical ectodermal ridge (AER, the pseudo-stratified epithelium located at the tip of the limb, required for normal limb bud outgrowth) (Fig. 5 *A* and *B*). Maximal interference with limb outgrowth was observed when embryos were injected at stages 13–17. In 35% of the experiments performed at this stage, truncation occurred in the most distal elements, showing absence of digits, carpals, and metacarpals (Fig. 5 *C* and *D*). In the majority of cases (65%), however, reduction in size and malformation of the tibia and fibula are observed (Fig. 5 *E* and *F*). Misexpression before stage 13 caused alteration, but not truncation, in 12% of the cases; misexpression of *DIO-1* after stage 18 reduced malformation frequency to 40%, and no truncations were observed. These data indicate that to affect the phenotype of the developing limb bud, *DIO-1* must be expressed in a permissive environment and is not the consequence of nonspecific toxic effects. Finally, we analyzed the caspase activity level in the developing limbs. The maximal effects of *DIO-1* appear to correlate with maximum caspase activity (not shown), reinforcing the view that execution of the death program by *DIO-1* is caspase dependent, although *DIO-1* overexpression precedes caspase activity.

Because misexpression of *DIO-1* can perturb AER formation, we would expect this process to be preceded by changes in gene expression, in both the ectoderm and the underlying limb bud mesoderm. *In situ* hybridization of embryos infected with the *RCAS-DIO-1* construct by using riboprobes for me-

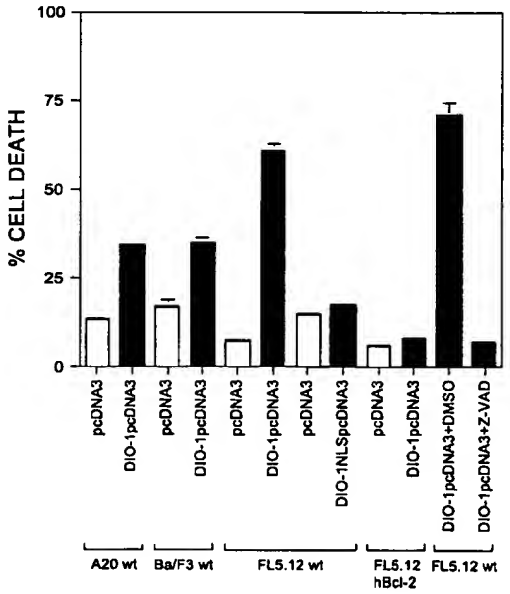

FIG. 3. *DIO-1* induces apoptosis *in vitro*. The *DIO-1* ORF was cloned into the pcDNA3 mammalian expression vector (Invitrogen). Both empty vector and the *DIO-1* construct were transiently transfected by electroporation into A20 and Ba/F3 cell lines. After 48-hr expression, the cells were permeabilized and stained with propidium iodide and cell cycle analyzed by FACS. FL5.12 wild-type and stably transfected hBcl-2 cells were transiently transfected as before. DIO-1NLSpcDNA3 encodes a mutant protein lacking amino acids 162–192, which is therefore unable to translocate to the nucleus. Where indicated, the general caspase inhibitor Z-VAD-fmk (50 μM final concentration; Bachem) was added immediately after transfection.

FIG. 4. Whole-mount *in situ* hybridization showing *DIO-1* expression pattern during murine development. Staining is shown of a 10.5-day mouse embryo and a 12.5-day mouse embryo limb (*Inset*).

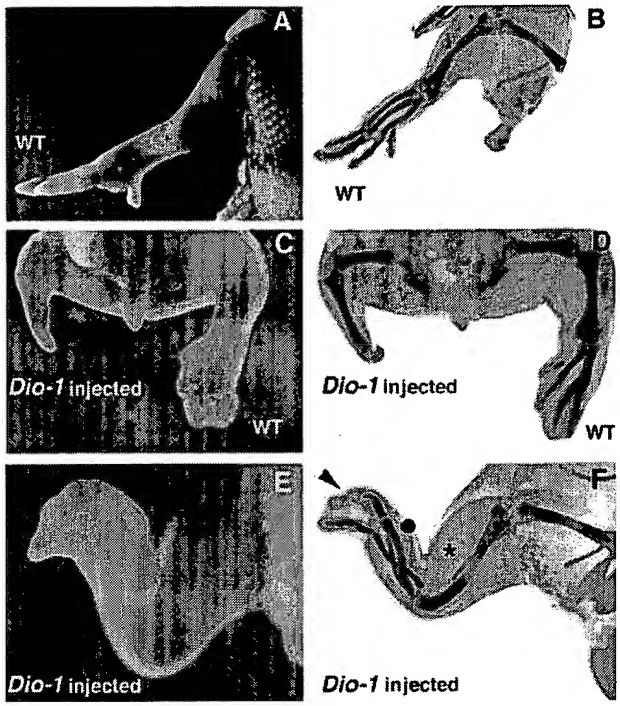

FIG. 5. *DIO-1* overexpression inhibits chicken limb outgrowth. A retroviral vector containing the *RCAS-DIO-1* construct was injected into limb primordia of stage 8–12 chicken embryos. Embryos were examined at different stages after infection. (*A*) Whole-mount preparation showing the hind limb of a wild-type embryo. (*B*) Alcian green staining of the same limb to visualize the normal cartilage pattern. (*C*) An infected embryo 6 days after injection, showing extensive truncation of the distal elements of the leg. (*D*) The same embryo after cartilage staining. Note the complete absence of elements distal to the tibia–fibula joint. (*E* and *F*) Whole- mount and cartilage staining of an embryo 8 days after infection with the *RCAS-DIO-1* construct. The infected limb is distorted and reduced in size, exhibiting an absence, reduction or malformation of phalanges, tarsals, and metatarsals (dot). In a few cases, the fibula was reduced in size (asterisk).

sodermal genes involved in limb outgrowth, such as *Msx-1* (Fig. 6*A*), *Lhx*-2 (Fig. 6*C*), and *NF-κB* (Fig. 6*D*), showed down-

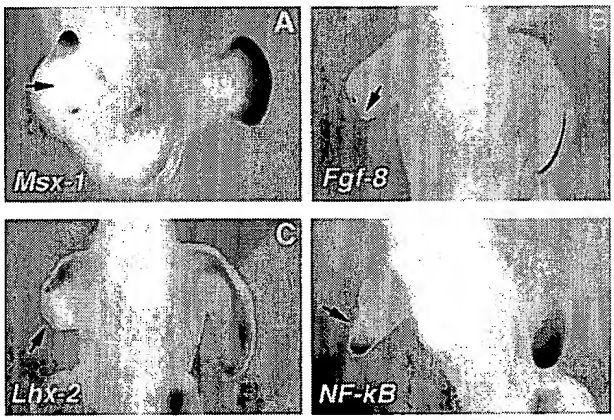

FIG. 6. *DIO-1* overexpression alters gene expression in the developing chicken limb bud. Misexpression of the *RCAS-DIO-1* construct leads to arrested limb outgrowth, preceded by changes in the expression of genes involved in outgrowth of the limb. Note the reduced size of the infected limb buds (left limb buds in all cases). Transcripts for *Msx-1* (*A*) *Fgf-8;* (*B*) *Lhx-2;* (*C*) and *NF-κB* (*D*) are strongly down-regulated (arrows) in the injected limb buds (compare with the normal expression pattern in the uninjected limb bud, right limb bud in all cases).

regulation in their transcript levels. Transcripts for ectodermal genes involved in limb outgrowth, such as *Fgf-8*, are also absent or down-regulated (Fig. 6*B*). It is not known whether *DIO-1* misexpression is directly responsible for the down-regulation of ectodermal gene markers (i.e., *Fgf-8*), or if this is a consequence of the previously altered mesodermal gene expression. The combination of these results indicates that *DIO-1* may be important during limb development, and its apoptotic function may be a driving force in sculpting the final structure.

DISCUSSION

The apoptotic pathway is still elusive and, in many cases, depends on the outcome of the balance between levels of survival and apoptotic genes, at either the transcriptional or translational level. Here we report the cloning and characterization of a gene involved in apoptosis, which is up-regulated under certain apoptotic conditions that do not involve p53-mediated cell death. This up-regulation is observed quite early in cell death kinetics and always before any of the classical characteristics of apoptosis, i.e., DNA laddering, haploid subG_0/G_1 cell-cycle peak, or alteration of cell membrane polarity, can be detected. This indicates that *DIO-1* acts very early in the apoptotic cascade and suggests a key role in the control of the initiating triggering mechanism. This gene is a putative transcription factor, based on its sequence analysis, which may have a role in regulating the cell death process at the transcriptional level. Other genes with similar characteristics have been reported, including p53 (34), c-myc (16), or members of the glucocorticoid receptor family (35). Our studies demonstrate that *DIO-1* overexpression induces massive cell death, which can be blocked through overexpression of hBcl-2, known to inhibit caspase activity (36–39). This indicates that *DIO-1* is upstream of the caspase cascade and that the induction of apoptosis driven by this gene proceeds through the main apoptotic route described so far. The Z-VAD-fmk blockade of *DIO-1*-induced apoptosis supports these conclusions.

The apoptotic mechanism activated by *DIO-1* requires its translocation to the nucleus; this finding, as well as its sequence and differential localization in living and apoptotic cells, can be used to draw inferences on its mode of function. *DIO-1* may thus be associated in the cytoplasm to a protein that prevents its entry into the nucleus, to which it must presumably be translocated to activate downstream mechanisms that initiate a caspase-executed apoptotic pathway. Such a mechanism is used by the nuclear transcription factor NF-κB, which is maintained as a complex with IκB in the cytoplasm until a given stimulus activates a caspase, leading to IκB phosphorylation, ubiquitination, and degradation, releasing the NF-κB proteins to traverse to the nucleus and activate gene transcription. A similar mechanism has been proposed for control of caspase-activated DNase and its translocation to the nucleus (7, 8).

To understand the *in vivo* role of this gene, we used the developing limb as a model. This system, which has been thoroughly characterized by developmental biologists, uses interference with limb outgrowth through modification of the gene expression pattern to analyze genes implicated in cell death. Here we have demonstrated that *DIO-1* affects chicken limb formation by general disruption of growth.

Limb buds infected with *DIO-1* constructs were reduced in size and failed to develop a defined AER. Severely truncated limbs with deformed and/or absent zeugopodal elements (most commonly the radius) and missing digits were also observed. After budding, continued limb outgrowth depends on correct AER formation. The reduced limb buds observed after *DIO-1* expression closely resemble the limb buds obtained after AER removal. All together, our experiments suggest that *DIO-1* overexpression perturbs maintenance of

AER function and hence limb outgrowth. Interestingly, the phenotypic changes caused by *DIO-1* misexpression kinetics, which result in altered limb development, appear to require the presence of the caspase activity required for elimination of interdigiting webs. *Fgf-8*, an AER-restricted gene involved in initiation and maintenance of limb outgrowth, is down-regulated or absent in infected limb buds, as are transcripts for *Msx-1* and *Lhx-2* genes involved in limb outgrowth whose expression is regulated by NF-κB. It thus appears that allowing DIO-1 protein translocation to the nucleus, down-regulation is observed for both mesodermal- and ectodermal-specific gene expression. It is unclear, however, whether this down-regulation occurs primarily in the mesoderm and indirectly in the AER or, alternatively, whether down-regulation of gene expression occurs initially in the AER and subsequently in the mesoderm. Identification of the mechanisms of action of *DIO-1* may be instrumental in answering this question and may provide another missing link in the identification of the mechanism that controls cell proliferation and cell death. In contrast to the consequences of *DIO-1* overexpression, ectopic NF-κB expression does not lead to significant morphological perturbations (data not shown). In sum, it appears that some proteins, such as NF-κB, control the cell proliferation and outgrowth of the vertebrate limb, whereas others, such as *DIO-1*, promote cell death. The integral process of limb outgrowth would thus require a balanced interaction between both forces.

We thank Drs. R. S. Geha, M. Izquierdo, D. Green, and J. Hurlé for reading the manuscript and C. Mark for editorial assistance. This work was funded in part by a grant from the Dirección General de Educación Superior e Investigación (DGESI) (Spain). D.G.-D. is the recipient of a fellowship from the Spanish Ministerio de Educación y Ciencia. The Department of Immunology and Oncology, Centro Nacional de Biotecnología, Universidad Autónoma, Madrid, was founded and is supported by the Spanish Research Council (CSIC) and Pharmacia & Upjohn.

1. Jacobson, M. D., Weil, M. & Raff, M. C. (1997) *Cell* **88,** 347–354.
2. Raff, M. C., Barres, B. A., Burne, J. F., Coles, H. S., Ishizaki, Y. & Jacobson, M. D. (1993) *Science* **262,** 695–700.
3. Vucic, D., Kaiser, W. J., Harvey, A. J. & Miller, L. K. (1997) *Proc. Natl. Acad. Sci. USA* **94,** 10183–10188.
4. Irmler, M. Thome, M., Hahne, M., Scheider, P., Hofmann, K., Steiner, V., Bodmer, J.-L., Schröter, M., Burns, K., Mattmann, C., *et al.* (1997) *Nature (London)* **388,** 190–195.
5. Ghayur, T., Banerjee, S., Hugunin, M., Butler, D., Herzog, L., Carter, A., Quintal, L., Sekut, L., Talanian, R., Paskind, M., *et al.* (1997) *Nature (London)* **386,** 619–623.
6. Izquierdo, M., Grandien, A., Criado, L. M., Robles, S., Leonardo, E., Albar, J. P., González de Buitrago, G. & Martínez-A, C. (1999) *EMBO J.* **18,** 156–166.
7. Enari, M., Sakahira, H., Yokoyama, H., Okawa, K., Iwamatsu, A. & Nagata, S. A. (1998) *Nature (London)* **391,** 43–50.
8. Sakahira, H., Enari, M. & Nagata, S. (1998) *Nature (London)* **391,** 96–99.
9. Clavería, C., Albar, J. P., Buesa, J. M., Barbero, J. L., Martínez-A, C. & Torres, M. (1998) *EMBO J.* **17,** 7199–7208.
10. Martin, D. P., Schmidt, R. E., DiStefano, P. S., Lowry, O. H., Carter, J. G. & Johnson, E. M., Jr. (1988) *J. Cell Biol.* **106,** 829–844.
11. Schwartz, L. M., Kosz, L. & Kay, B. K. (1990) *Proc. Natl. Acad. Sci. USA* **87,** 6594-6598.
12. Wagner, A. J., Kokontis, J. M. & Hay, N. (1994) *Genes Dev.* **8,** 2817–2830.
13. Chong, L. E-C., Chan, F. K-M., Cado, D. & Winoto, A. (1997) *EMBO J.* **16,** 1865–1875.
14. Cohen, J. J. & Duke, R. C. (1984) *J. Immunol.* **132,** 38–42.
15. Kumar, A., Commane, M., Flickinger, T. W., Horvath, C. M. & Stark, G. R. (1997) *Science* **278,** 1630–1632.
16. Evan, G. I., Wyllie, A. H., Gilbert, C. S., Littlewood, T. D., Land, H., Brooks, M., Waters, C. M., Penn, L. Z. & Hancock, D. C. (1992) *Cell* **69,** 119–128.
17. Ham, J., Babij, C., Whitfield, J., Pfarr, C. M., Lallemand, D., Yaniv, M. & Rubin, L. L. (1995) *Neuron* **14,** 927–939.
18. Baichwal, V. R. & Baeuerle, P. A. (1997) *Curr. Biol.* **7,** 94–96.
19. White, K., Grether, M. E., Abrams, J. M., Young, L., Farrell, K. & Steller, H. (1994) *Science* **264,** 677–683.
20. Grether, M. E., Abrams, J. M., Agapite, J., White, K. & Steller, H. (1995) *Genes Dev.* **9,** 1694–1708.
21. Chen, P., Nordstrom, W., Gish, B. & Abrams, J. M. (1996) *Genes Dev.* **10,** 1773–1782.
22. Kanegae, Y., Tavares, A. T., Izpisúa Belmonte, J. C. & Verma, I. M. (1998) *Nature (London)* **392,** 611–614.
23. Sambrook, J., Fritsch, E. F. & Maniatis, T. (1989) in *Molecular Cloning: A Laboratory Manual*, 2nd Ed. (Cold Spring Harbor Lab. Press, Plainview, NY).
24. Wilkinson, D. G. (1993) in *In Situ Hybridisation*, ed. Wilkinson, D. G. (Oxford Univ. Press, Oxford).
25. Izpisúa Belmonte, J. C., De Robertis, E. M., Storey, K. G. & Stern, C. (1993) *Cell* **74,** 645–659.
26. Robert, B., Lyons, G., Simandl, B-K., Kuroiwa, A. & Buckingham, M. (1991) *Genes Dev.* **5,** 2363–2374.
27. Vogel, A., Rodriguez, C. & Izpisúa Belmonte, J. C. (1996) *Development (Cambridge, U.K.)* **122,** 1737–1750.
28. Morgan, B. A., Izpisúa Belmonte, J. C., Duboule, D. & Tabin, C. J. (1992) *Nature (London)* **358,** 236–239.
29. Liang, P. & Pardee, A. B. (1992) *Science* **257,** 967–971.
30. Altschul, S. F., Gish, W., Miller, W., Myers, E. W. & Lipman, D. J. (1990) *J. Mol. Biol.* **215,** 403–410.
31. Kozak, M. (1987) *Nucleic Acids Res.* **15,** 8125–8148.
32. Brás, A., Ruiz-Vela, A., González de Buitrago, G. & Martínez-A, C. (1999) *FASEB J.* **13,** 931–944.
33. Schwabe, J., Rodriguez-Esteban, C. & Izpisúa Belmonte, J. C. (1998) *Trends Genet.* **14,** 229–235.
34. Polyak, K., Xia, Y., Zweir, J. L., Kinzler, K. W. & Vogelstein, B. (1997) *Nature (London)* **389,** 300–305.
35. Tolosa, E., King, L. B. & Ashwell, J. D. (1998) *Immunity* **8,** 67–76.
36. Kluck, R. M, Bossy-Wetzel, E., Green, D. R. & Newmeyer, D. D. (1997) *Science* **275,** 1132–1136.
37. Adams, J. M. & Cory, S. (1998) *Science* **281,** 1322–1325.
38. Huang, D., Adams, J. M. & Cory, S. (1998) *EMBO J.* **17,** 1029–1039.
39. Cuende, E., Ales-Martínez, J. E., Ding, L., González, M., Martínez-A, C. & Núñez, G. (1993) *EMBO J.* **12,** 1555–1560.

MOLECULAR AND CELLULAR BIOLOGY, May 2003, p. 3216–3225 Vol. 23, No. 9
0270-7306/03/$08.00+0 DOI: 10.1128/MCB.23.9.3216–3225.2003

Death Inducer-Obliterator 1 Triggers Apoptosis after Nuclear Translocation and Caspase Upregulation

David García-Domingo, Dorian Ramírez,† Gonzalo González de Buitrago, and Carlos Martínez-A*

Department of Immunology and Oncology, Centro Nacional de Biotecnología/CSIC, Universidad Autonomo de Madrid, Campus de Cantoblanco, E-28049 Madrid, Spain

Received 22 July 2002/Returned for modification 4 September 2002/Accepted 4 February 2003

Death inducer-obliterator 1 (DIO-1) is a gene that is upregulated early in apoptosis. Here we report that in healthy cells, the DIO-1 gene product was located in the cytoplasm, where it formed oligomers. After interleukin-3 starvation or c-Myc-induced apoptosis in serum-free conditions, DIO-1 translocated to the nucleus, where it upregulated caspase levels and activity. A nuclear localization signal deletion mutant (DIO-1ΔNLS) was unable to translocate to the nuclear compartment in the absence of interleukin-3 and failed to upregulate procaspase levels or trigger cell death. In addition, cells stably expressing DIO-1ΔNLS were protected from apoptosis induced by interleukin-3 withdrawal. These results indicate that DIO-1 has a relevant role in regulating the early stages of cell death.

Apoptosis, or programmed cell death, has a major role in normal development, tissue homeostasis, defense against viral invasion, immune modulation, and, when dysregulated, modulation of autoimmune and clonal or neoplastic diseases (15, 17, 30). Apoptosis is characterized by cell shrinkage, chromatin condensation, internucleosomal DNA cleavage, membrane blebbing, and the formation of apoptotic bodies that are phagocytosed by other cells (8, 38). These morphological changes are orchestrated by the activity of a family of aspartate-specific proteases called caspases (4, 7, 34).

Caspases are produced in cells as catalytically inactive zymogens, or procaspases, composed of three subunits, a prodomain and two catalytic subdomains, known as the large and small subunits (1). Procaspases must be proteolytically processed to become active proteases. An effector caspase, for example caspase 3, is activated by an initiator caspase, such as caspase 9, through proteolytic cleavage at specific internal Asp residues to give rise to the two subunits of the mature caspase. Once activated, the effector caspases cleave a broad spectrum of cellular targets, leading ultimately to cell death (38). Activation of the initiator caspases is in turn regulated by upstream protein complexes. In the case of the so-called "extrinsic" pathway, activation of death receptors such as Fas/CD95 and tumor necrosis factor receptor 1 after binding of their respective ligands induces recruitment of caspase 8 (FLICE) via the adapter molecule FADD (Fas-associated protein with death domain) (27). Caspase 8 can activate effector caspases either directly (3, 27) or indirectly by cleaving Bid and inducing the release of mitochondrial cytochrome *c* (18, 25).

In the case of the "intrinsic" death receptor-independent pathway, apoptotic cell death is induced directly by death stimuli and is also regulated by adapter complexes. This is the case of one of the major routes to caspase activation pathways, triggered by cytochrome *c* release from the mitochondrial intermembrane space into the cytosol (23). Cytosolic cytochrome *c* promotes assembly of a protein complex called the apoptosome, which includes caspase 9 bound to the CED-4 homolog Apaf-1 (19, 42), inducing autoactivation of procaspase 9 (33, 37). Following activation, caspase 9 cleaves and activates procaspase 3 (19, 42), giving rise to a proteolytic cascade involving multiple caspases.

DIO-1 was identified by a differential display approach (21) in WOL-1 pre-B cells induced to undergo apoptosis by interleukin-7 (IL-7) starvation (9). Its predicted amino acid sequence showed transcriptional activation domains, a canonical bipartite nuclear localization signal (NLS), a PhD finger, and a carboxy-terminal lysine-rich region. DIO-1 mRNA was upregulated soon after apoptotic induction by several stimuli, including removal of IL-7, addition of dexamethasone or gamma interferon in WOL-1 cells, immunoglobulin M (IgM) receptor cross-linking in WEHI-231 cells, or c-*myc* activation under serum-free conditions in the absence of p53 expression in MEF(10.1)Val5MycER cells. Overexpression of DIO-1 in cells or misexpression in chick limbs induced massive apoptosis in the absence of any apoptotic stimuli; this could be inhibited by Bcl-2 overexpression or incubation with the general caspase inhibitor benzyloxycarbonyl-Val-Ala-Asp-fluoromethyl ketone (z-VAD-fmk). These results suggested that DIO-1-induced apoptosis requires caspase activation. Furthermore, overexpression of a DIO-1 deletion mutant lacking both NLSs failed to induce cell death, linking its lack of lethality to an inability to translocate.

Here we studied the mechanism by which DIO-1 induces apoptosis and the importance of its subcellular localization. We generated several tagged constructs and analyzed the subcellular distribution pattern of both wild-type and mutant DIO-1 in various apoptotic situations, revealing nuclear translocation as the main regulatory event in the DIO-1-activated apoptotic pathway. We provide evidence that DIO-1 translocation boosts the apoptotic machinery by upregulating protein

* Corresponding author. Mailing address: Department of Immunology and Oncology, Centro Nacional de Biotecnología/CSIC, UAM Campus de Cantoblanco, E-28049 Madrid, Spain. Phone: 34 91 585 45 59. Fax: 34 91 372 04 93. E-mail: cmartineza@cnb.uam.es.

† Present address: University of Michigan Medical School, Ann Arbor, MI 48109.

levels of procaspase 3 and 9, which enhances their apoptosis-inducing activity.

MATERIALS AND METHODS

Expression plasmids. DIO-1ΔNLSpcDNA3 was generated from DIO-1 cloned in pcDNA3 by reverse PCR with the circular plasmid as the template and the primers 5′-GAAGATTCTGCCGAAACTGGG-3′ and 5′-AAGTTCCTTC AACGTAAGG-3′, which span the NLSs and the connecting sequence; the PCR product was permitted to further self-ligate. Both N-terminally Flag-tagged DIO-1 and DIO-1ΔNLS were PCR amplified from their corresponding pcDNA3 constructs with a proof-reading polymerase and the primers 5′-GCGGATCCG ATGATAAAGGGCACCTG-3′ and 5′-CGACCTCGAGTTACCAAGGCCTA AAACTG-3′ for in-frame reading. The PCR products were digested with *Bam*HI and *Xho*I and subcloned into the pCMV-Tag 2B vector (Stratagene). DIO-1/Myc was generated similarly after PCR amplification with the primers 5′-TGGAATTCCACCATGGATGATAAAGGGCAC-3′ and 5′-GCTCTAGA CCAAGGCCTAAAACTG-3′ from DIO-1pcDNA3, digested with *Eco*RI and *Xba*I, and subcloned into the pEF4/*Myc*-His A vector (Invitrogen). All constructs were verified by nucleotide sequencing.

Cell culture. FL5.12 and MEF(10.1)Val5MycER cells were cultured as described previously (9). 293T cells were cultured in Dulbecco's modified Eagle's medium supplemented with 10% fetal bovine serum, 2 mM L-glutamine, and antibiotics.

Antibodies and reagents. Production of the polyclonal antibody against murine DIO-1 amino acids 58 to 72 has been described (9). Polyclonal rabbit anti-mouse caspase 3 was the kind gift of T. Mak and R. Hakem (Ontario Cancer Institute, Toronto, Canada); anti-caspase 9 was the kind gift of D. R. Green and B. Wolf (39). Anti-Flag M2 monoclonal antibody (Sigma), anti-Myc 9E10 monoclonal antibody (Santa Cruz Biotechnologies), protein A-agarose (Sigma), protein G-agarose (Sigma), antiphosphoserine sampler kit (Biomol), antiphosphoserine monoclonal antibody (Calbiochem), and antiphosphothreonine monoclonal antibody (Calbiochem) were purchased as indicated. z-VAD-fmk was purchased from Bachem.

Establishment of FL5.12 cells stably overexpressing DIO-1ΔNLS. FL5.12 cells (3×10^6) were electroporated with 10 μg of DIO-1ΔNLS construct or pcDNA3. Transfected cells were resuspended in 48 ml of complete medium and distributed in a 48-well plate. Selection was performed after 24 h by removing the medium and adding fresh complete medium containing 1 mg of G418 per ml. Selection was carried out for 30 days, and DIO-1ΔNLS expression was determined by reverse transcription-PCR and Western blotting.

Subcellular fractionation. FL5.12 cells (2×10^7) were harvested and washed in ice-cold phosphate-buffered saline (PBS), and pellets were resuspended in 5 volumes of ice-cold buffer A (10 mM HEPES [pH 8.0], 0.5 M sucrose, 1 mM EDTA, 0.5 mM spermidine, 0.15 mM spermine, 15 mM KCl, 0.5 mM dithiothreitol, 10 μg of aprotinin per ml, 10 μg of pepstatin A per ml, 10 μg of leupeptin per ml, 1 mM phenylmethylsulfonyl fluoride [PMSF], 100 μM Na_3VO_4, and 10 mM NaF). After incubation on ice for 15 min, cells were lysed by three freeze-thaw cycles and centrifuged (1,000 × *g*, 10 min, 4°C), and the nuclear pellet was resuspended in buffer B (10 mM piperazine-*N*,*N*′-bis(2-ethanesulfonic acid) [PIPES, pH 7.4], 80 mM KCl, 20 mM NaCl, 5 mM sodium EGTA, 250 mM sucrose, 1 mM dithiothreitol, 10 μg of aprotinin per ml, 10 μg of pepstatin A per ml, 10 μg of leupeptin per ml, 1 mM PMSF, 100 μM Na_3VO_4, and 10 mM NaF) at 8.5×10^7 nuclei/ml. Samples were separated by sodium dodecyl sulfate-polyacrylamide gel electrophoresis (SDS-PAGE) under reducing conditions. Purity of the cytosolic and nuclear fractions was tested by Western blotting with compartment-specific antibodies to procyclic acidic repetitive protein and calpain-1 (not shown).

Transfections and immunoprecipitation. Transient transfections in FL5.12 and MEF(10.1)Val5MycERcells were performed by electroporation as described previously (9). 293T cells were transiently transfected in six-well plates with Lipofectamine Plus (Life Technologies) following the manufacturer's protocol. Cytosolic extracts for immunoprecipitation were obtained after cell lysis in NP-40 buffer (40 mM Tris-HCl [pH 8], 500 mM NaCl, 0.1% NP-40, 6 mM EDTA, 6 mM EGTA, 10 μg of aprotinin per ml, 10 μg of pepstatin A per ml, 10 μg of leupeptin per ml, 1 mM PMSF, 100 μM Na_3VO_4, and 10 mM NaF) or a digitonin-containing buffer (10 mM triethanolamine [pH 8], 150 mM NaCl, 1 mM EDTA, 10% glycerol, 1% digitonin, 10 μg of aprotinin per ml, 10 μg of pepstatin A per ml, 10 μg of leupeptin per ml, 1 mM PMSF, 100 μM Na_3VO_4, and 10 mM NaF). Immunoprecipitation was performed by preclearing lysates with 30 μl of protein A/G-agarose (1 h, 4°C, with gentle rotation), followed by incubation with the appropriate antibody (10 μg/ml; 1 h, 4°C). After addition of protein A- or protein G-agarose (30 μl), beads were pelleted by brief centrifugation and washed three times in 50 mM Tris-HCl (pH 7.6) buffer, and the pellet was boiled in loading buffer and analyzed in Western blot.

Phosphatase treatment. 293T cells transiently transfected with Flag-tagged DIO-1 were harvested, washed in ice-cold PBS, and lysed in a digitonin-containing buffer (40 mM Tris-HCl [pH 8], 50 mM NaCl, 2 mM $MnCl_2$, 1% digitonin, 10 μg of aprotinin per ml, 10 μg of pepstatin A per ml, 10 μg of leupeptin per ml, 1 mM PMSF). After removal of cellular debris by centrifugation, lysates were treated with 500 U of λ-phosphatase (Calbiochem) (30 min, 30°C). The reaction was terminated by addition of loading buffer and then analyzed in Western blot.

Western blot analysis. Cells for analysis of procaspase expression were washed with PBS, and the pellet was suspended in lysis buffer (137 mM NaCl, 20 mM Tris-HCl [pH 8], 1 mM $MgCl_2$, 1 mM $CaCl_2$, 10% glycerol, 1% NP-40, 0.5% deoxycholate, 0.1% SDS, 10 μg of aprotinin per ml, 10 μg of pepstatin A per ml, 10 μg of leupeptin per ml, and 1 mM PMSF) for 30 min on ice. The protein content of the lysates was quantified with the Bio-Rad DC protein assay (Bio-Rad); after SDS-PAGE, proteins were transferred to nitrocellulose membranes (Bio-Rad). Equal protein loading was verified by Ponceau Red (Sigma) staining. Membranes were blocked overnight with 5% nonfat dry milk in TBS buffer (20 mM Tris-HCl [pH 7.5], 150 mM NaCl); subsequent incubations and membrane washes were performed in TBS-T buffer (20 mM Tris-HCl [pH 7.5], 150 mM NaCl, and 0.2% Tween 20) containing 1% nonfat dry milk. After 2 h of antibody incubation and 1 h of washing, blots were developed with peroxidase-conjugated anti-rabbit or anti-mouse immunoglobulin antibodies (Dako), and proteins were detected by an enhanced chemiluminescence system (ECL; Amersham).

Fluorescence microscopy. For immunofluorescence, cells were cultured on coverslips, washed in PBS, fixed in 4% paraformaldehyde (15 min, room temperature), washed three times in PBT (PBS with 0.1% Tween 20), incubated in 2% bovine serum albumin, and incubated for 1 h with anti-DIO-1 (1:100) or anti-Flag M2 (1:500) in PBT. After incubation, cells were washed three times in the same buffer and incubated for 1 h with indocarbocyanine-conjugated secondary antibodies (Jackson ImmunoResearch). After washing, samples were incubated with Sybr Green (Molecular Probes) in PBS for DNA staining. Serial Z-sections were obtained with an Ar-Kr laser and a TCS-NT Leica confocal imaging system.

Enzyme assay for caspase activity. Cells were collected, washed with ice-cold PBS, and resuspended in extraction buffer (50 mM Tris-HCl [pH 7.6], 150 mM NaCl, 0.5 mM EDTA, 10 mM NaH_2PO_4, 10 mM Na_2HPO_4, 1% Nonidet P-40, 0.4 mM Na_3VO_4, 1 mM PMSF, 10 μg of aprotinin per ml, 10 μg of pepstatin A per ml, 10 μg of leupeptin per ml). After incubation (30 min, on ice), the cell lysate was centrifuged (20,000 × *g*, 30 min), and the supernatant was used as the cytosolic extract. Five micrograms of cytosolic proteins, estimated by the bicinchoninic acid method (36), were diluted fivefold in assay buffer (25 mM HEPES [pH 7.5], 0.1% CHAPS, 10% sucrose, 10 mM dithiothreitol, and 0.1 mg of ovalbumin per ml) and incubated (1 h, 37°C) with 10 μM of the fluorescent substrate Ac-DEHD-AMC (acetyl-Asp-Glu-His-Asp-7-amino-4-methylcoumarin), Ac-DEVD-AMC (acetyl-Asp-Glu-Val-Asp-7-amino-4-methylcoumarin), Ac-VEID-AMC (acetyl-Val-Glu-Ile-Asp-7-amino-4-methylcoumarin), or Ac-LEHD-AMC (acetyl-Leu-Glu-His-Asp-7-amino-4-methylcoumarin) to measure caspase 2, caspase 3-like, caspase 6, and caspase 9 activity, respectively. The reaction was terminated by addition of high-pressure liquid chromatography (HPLC) buffer (water-acetonitrile [75:25], 0.1% trifluoroacetic acid). Cleaved substrate fluorescence was determined by C_{18} reverse-phase HPLC with fluorescence detection (338 nm excitation, 455 nm emission). Control experiments confirmed linearity with time and protein concentration of substrate release.

Apoptosis assay. Apoptosis was evaluated by staining cellular DNA content with the DNA intercalator propidium iodide in a semiautomatic procedure (DNA-Prep Reagents; Coulter), followed by analysis on an Epics XL flow cytometer (Coulter). Briefly, cells (10^5 to 10^6) were recovered by centrifugation, resuspended in 100 μl of PBS, permeabilized, and stained by adding 100 μl of detergent reagent followed by 1 ml of propidium iodide solution. After mixing, samples were incubated (37°C, 1 h) and analyzed by flow cytometry.

RESULTS

DIO-1 nuclear translocation following apoptotic stimulation requires the NLS. We previously reported differences in DIO-1 mRNA levels after induction of p53-dependent and -independent apoptosis in MEF(10.1)Val5MycER cells (9). DIO-1 transcripts were upregulated in apoptotic processes in a p53-independent fashion. The presence of two putative NLSs in the DIO-1 gene product suggested that it may be localized

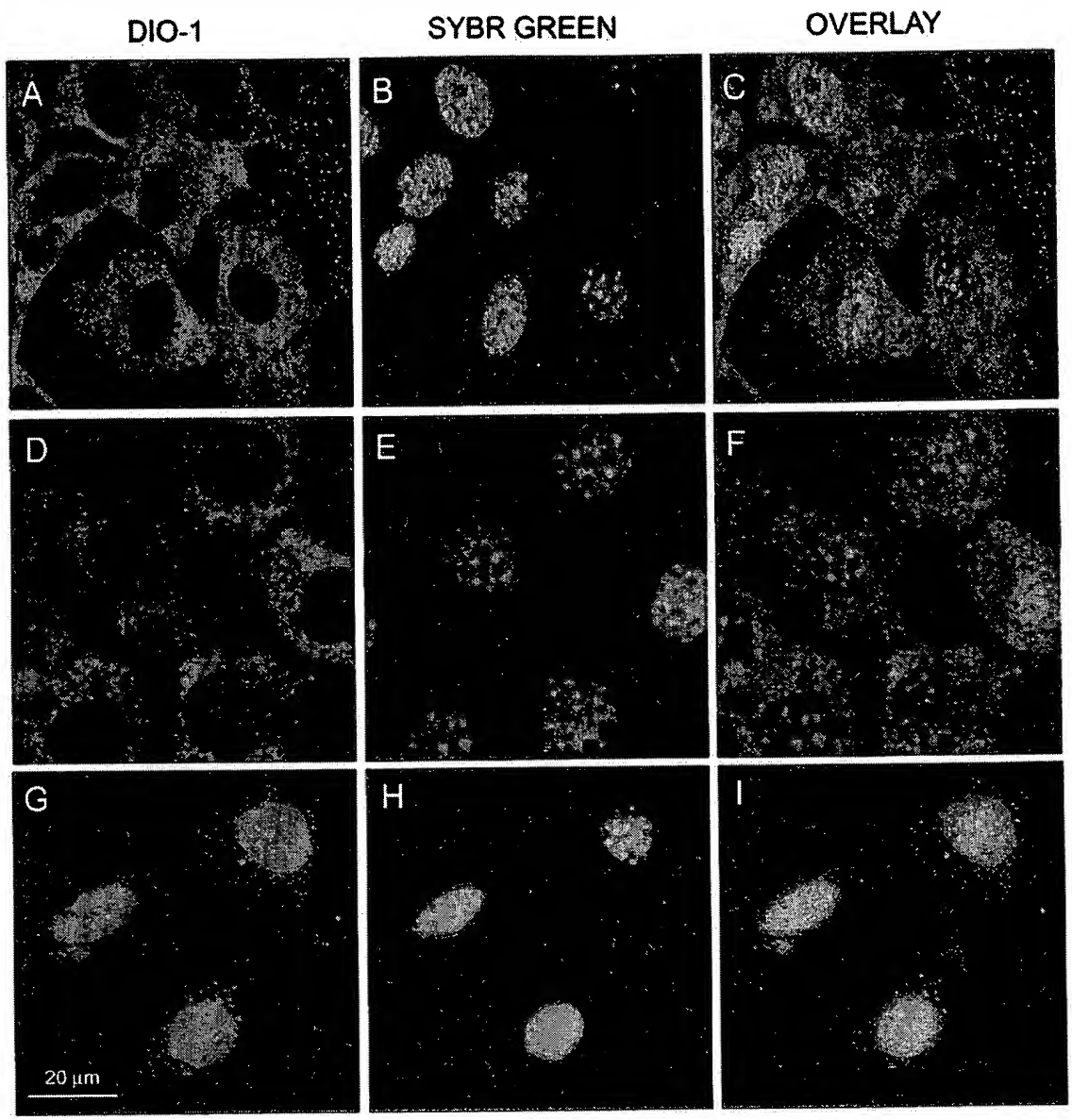

FIG. 1. Immunolocalization of endogenous DIO-1 under apoptotic conditions. (A to C) Viable (nonapoptotic) MEF(10.1)Val5MycER cells were stained with anti-DIO-1 antibody (red); nuclei were stained with Sybr Green (green). (D to F) The same cells were induced to apoptosis by lowering the incubation temperature (32°C, 12 h) to activate p53 in the presence of 17β-estradiol (1 μM). Note the clear cytoplasmic pattern of DIO-1, although some cells have already begun the apoptotic program. (G to I) The same cell line, incubated at 39°C to inactivate p53, was 17β-estradiol treated (1 μM) and serum starved for 8 h, the time at which DIO-1 mRNA is upregulated. Note nuclear translocation of DIO-1 to the intact, nonapoptotic nuclei.

in the nucleus (9). To study its putative role as a transcription factor, we examined the subcellular localization pattern of the DIO-1 gene product and its NLS deletion mutant (DIO-1ΔNLS). Immunofluorescence microscopy of healthy MEF(10.1)Val5MycER cells with an affinity-purified rabbit antiserum specific for a DIO-1 peptide (9) indicated a clear cytoplasmic pattern for the DIO-1 protein, which was nearly absent in the nucleus (Fig. 1A to C). p53-mediated triggering of apoptosis showed no change in the DIO-1 localization pattern (Fig. 1D to F), although the cells underwent apoptosis (not shown). Cells cultured at 39°C to inactivate p53, then induced to apoptosis by 17β-estradiol addition and fetal bovine serum starvation, showed DIO-1 translocation from cytoplasm to the nucleus (Fig. 1G to I). This was observed before cell death was detectable by any method and in parallel to mRNA upregulation kinetics.

We examined the subcellular localization of the DIO-1ΔNLS mutant, but as the anti-DIO-1 antibody recognizes both wild-type and mutant proteins, the mutant was Flag tagged (DIO-1ΔNLS/Flag) and transiently transfected into MEF(10.1)Val5MycER cells. Apoptosis was induced 24 h post-transfection, and staining was performed at the same time

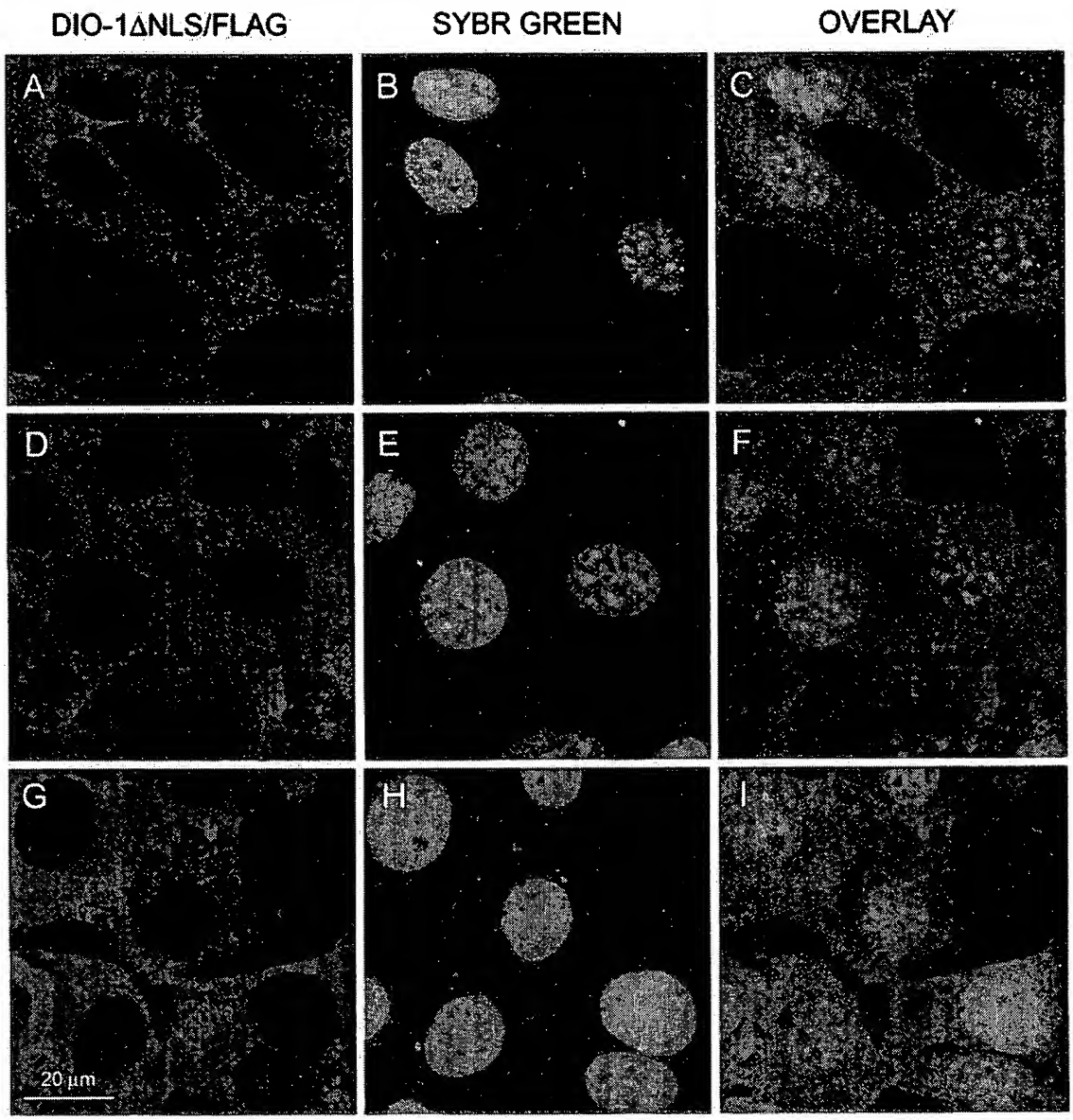

FIG. 2. Immunolocalization of DIO-1ΔNLS in MEF(10.1)Val5MycER cells under apoptotic conditions. A DIO-1ΔNLS Flag-tagged construct was transiently transfected into the cells, which were analyzed 36 h posttransfection. A selected field of positive cells is shown. (A to C) Viable cells were stained with anti-Flag antibody (red) and Sybr Green (green). (D to F) Conditions as for Fig. 1D to F. (G to I) Conditions as for Fig. 1G to I. The protein did not translocate to the nucleus in the presence of the stimulus that induced wild-type DIO-1 translocation.

points as for wild-type DIO-1. A clear cytoplasmic pattern was observed in healthy cells (Fig. 2A to C) and in those undergoing p53-induced apoptosis (Fig. 2D to F). DIO-1ΔNLS was unable to translocate to the nucleus under conditions that promoted translocation of the wild-type form (Fig. 2G to I), as predicted by its lack of NLS.

DIO-1 forms oligomers. To test for the association state of DIO-1, we fused murine DIO-1 to N-terminal Flag (DIO-1/Flag) and C-terminal Myc (DIO-1/Myc) tags in different constructs. The constructs were coexpressed by transient transfection into human embryonic kidney 293T cells, and proteins were isolated under nondenaturing conditions with buffers that permitted cytosolic extraction. Western blot analysis with the anti-DIO-1 antibody (Fig. 3A) and antitag antibodies (Fig. 3B) confirmed expression in total lysates of cells transfected with the appropriate plasmids, but not in cells transfected with control plasmids. In all cases, a triplet was observed with very close bands. The triplets do not correspond to proteolytic degradation products, as they were detected equally well with antibodies to tags located at both ends of the protein, in the presence of large amounts of protease inhibitors. These multiple bands are more likely to represent posttranslational modifications of DIO-1.

Oligomerization was determined in an immunoprecipitation assay performed with anti-Myc and resolved in SDS-polyacrylamide gel electrophoresis (SDS-PAGE). Subsequent Western

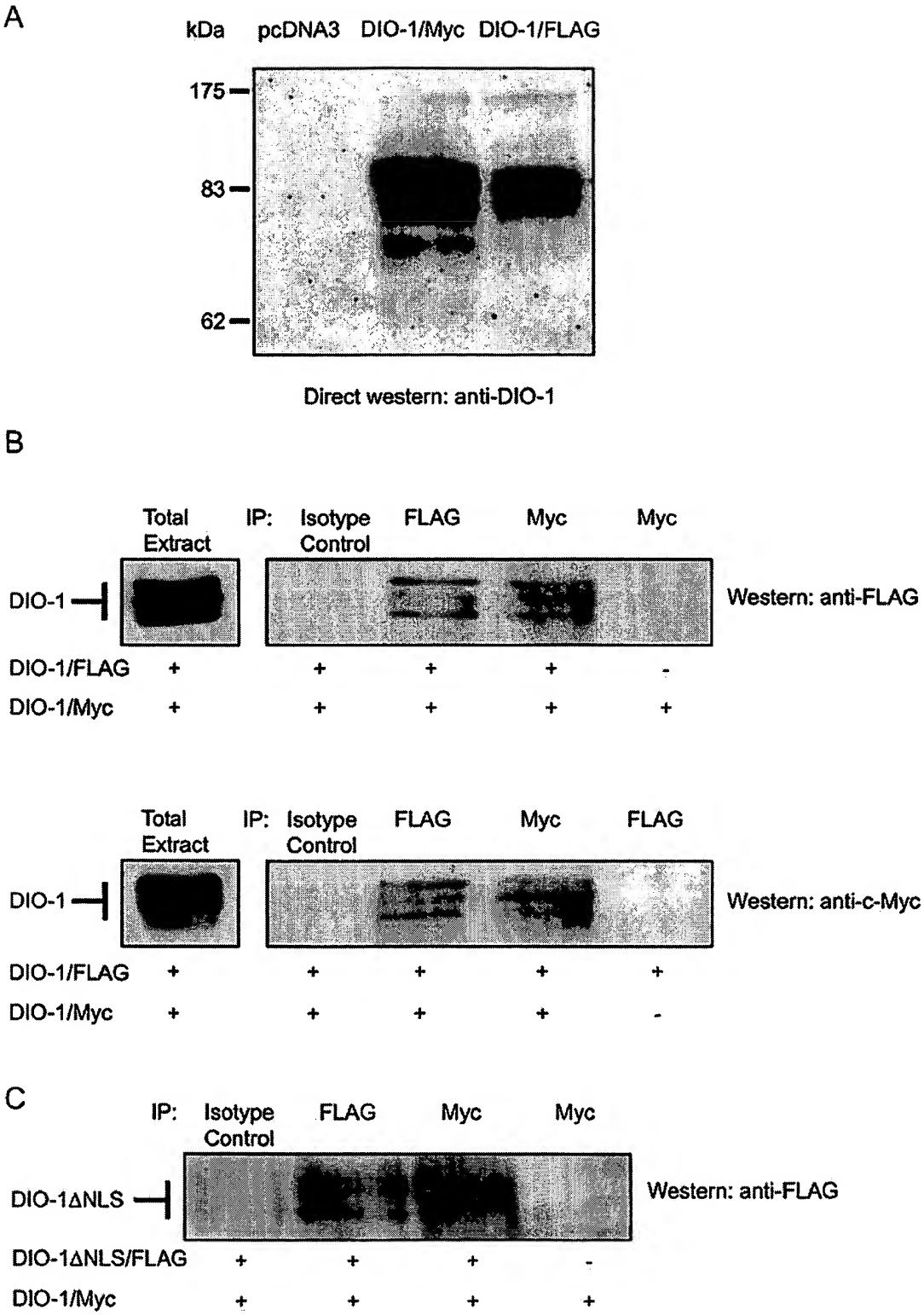

FIG. 3. DIO-1 forms oligomers. (A) Expression of DIO-1 gives rise to a three-band pattern in Western blot. Whole-cell extracts from 293T cells transfected with vector plasmid (pcDNA3) or expression plasmids encoding Myc- or Flag-tagged DIO-1 were analyzed in Western blot with the anti-DIO-1 antibody. Molecular size markers are indicated at the left. (B) 293T cells were cotransfected with constructs encoding Myc- and Flag-tagged DIO-1 except for the last lane, in which only one construct was transfected as a negative immunoprecipitation control. After 48 h, extracts were immunoprecipitated with anti-Flag or anti-Myc monoclonal antibody. An irrelevant isotype-matched antibody was used as a control. Immunoprecipitates were analyzed by SDS-PAGE and blotted with anti-Flag (upper panel) or anti-Myc antibody (lower panel). Total cell extracts were also analyzed by SDS-PAGE and blotted with the same antibodies (left). (C) 293T cells were cotransfected with constructs encoding Myc-tagged DIO-1 and Flag-tagged DIO-1ΔNLS except for the last lane, in which only DIO-1/Myc was transfected. The experimental procedure was identical to that for panel B, upper panel. All results are representative of three independent experiments.

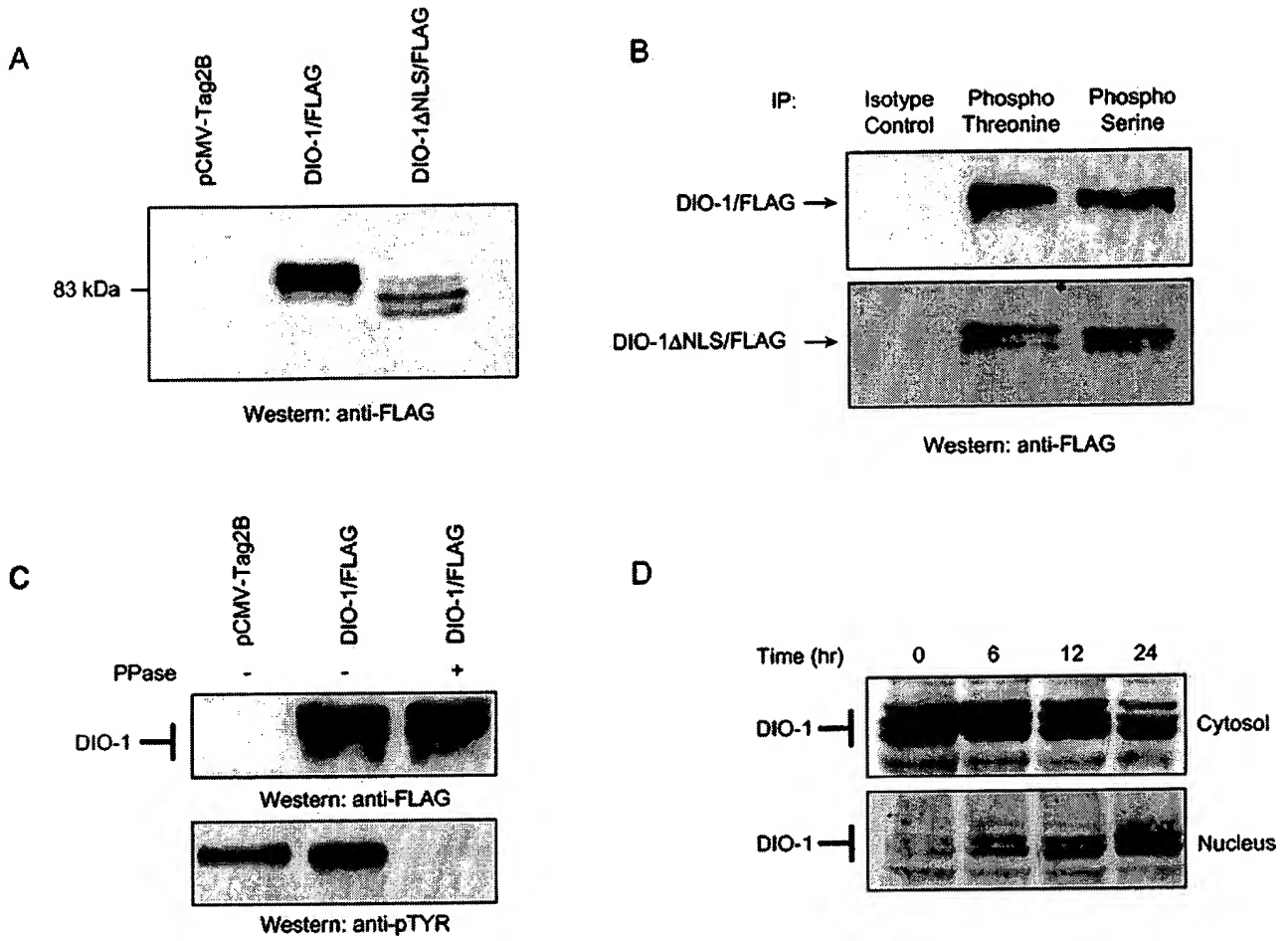

FIG. 4. DIO-1 is present in several forms with distinct subcellular distribution. (A) Western blot of lysates from 293T cells transfected with empty vector (pCMV-Tag2B), Flag-tagged DIO-1, or Flag-tagged DIO-1ΔNLS. The membrane was blotted with anti-Flag antibody. A representative result of five independent experiments is shown. Note the lower apparent molecular size of the deletion mutant and the three-band pattern. (B) 293T cells were transiently transfected with the indicated Flag-tagged constructs. Lysates were immunoprecipitated with antiphosphothreonine, antiphosphoserine, or an irrelevant control antibody and then blotted with anti-Flag monoclonal antibody. Only the upper and middle bands were detected. (C) 293T cells were transiently transfected with Flag-tagged DIO-1. Untreated or λ-phosphatase-treated lysates were separated by SDS-PAGE and then blotted with anti-Flag monoclonal antibody. Phosphatase treatment did not cause a mobility shift (upper panel). Dephosphorylation of total cellular proteins was verified by blotting with antiphosphotyrosine antibody (lower panel). (D) FL5.12 cells deprived of IL-3 for the times indicated were separated into cytosolic and nuclear fractions (Materials and Methods). Extracts were separated by SDS-PAGE and analyzed by Western blotting with the anti-DIO-1 antibody.

blotting with an anti-Flag antibody showed that DIO-1/Flag coimmunoprecipitated with DIO-1/Myc, whereas negative controls gave no bands (Fig. 3B). The amount of coprecipitated material was distributed equally among the three bands observed. To verify this interaction, we performed reciprocal experiments with anti-Flag to immunoprecipitate DIO-1/Flag, followed by blotting with anti-Myc. Concurring with the reverse experiment, DIO-1/Myc coimmunoprecipitated specifically with DIO-1/Flag (Fig. 3B). Similar experiments with DIO-1/Myc and DIO-1ΔNLS/Flag showed that both constructs coimmunoprecipitated (Fig. 3C), as confirmed by the reciprocal experiment (not shown). These results strongly suggest that DIO-1 homo-oligomerizes and that deletion of both NLS regions and their interspace does not affect this interaction. In addition, the C-terminal end of the protein is not needed for oligomerization, as glutathione *S*-transferase fusions lacking the terminal 86 amino acids interacted with endogenous DIO-1 (not shown). The exact oligomerization site nonetheless remains to be determined. Based on computer predictions, the lysine-rich region, which resembles part of the c-*myc* dimerization site, may contribute to DIO-1 oligomerization; experiments are under way to analyze this possibility.

DIO-1 is present in multiple forms with distinct subcellular localizations. Triplet banding in Western blot, rather than a single band, may be produced by different protein phosphorylation states. To study this, Flag-tagged DIO-1 and DIO-1ΔNLS were transiently transfected in 293T cells and immunoprecipitated with antiphosphoserine, antiphosphothreonine, and antityrosine antibodies. Expression of both constructs showed the predicted three-band pattern (Fig. 4A), although only the two upper bands immunoprecipitated with antiphosphoserine and antiphosphothreonine (Fig. 4B). The lowest

band was absent, suggesting that it corresponds to a protein that is not phosphorylated on serine/threonine, whereas the two upper bands appeared to correspond to phosphorylated forms. Antiphosphotyrosine antibodies did not immunoprecipitate DIO-1 (not shown). Phosphatase treatment of cell extracts did not result in the loss of the multiple bands (Fig. 4C), indicating that the mobility shift was not caused by phosphorylation alone. These results nonetheless show that DIO-1 is present in multiple forms that differ in electrophoretic mobility. Of these, the larger forms are phosphorylated on serine/threonine residues.

To determine the role of the different DIO-1 forms in apoptosis, we examined their subcellular distribution and appearance under apoptotic conditions. Apoptosis was induced in FL5.12 cells by IL-3 withdrawal. Samples were taken at several time points, and the cytosolic and nuclear fractions were separated by centrifugation, resolved in SDS-PAGE, and analyzed in Western blots with the anti-DIO-1 antibody (Fig. 4D). Healthy cells (lanes labeled 0 h) showed higher DIO-1 protein levels in the cytosol than in the nucleus, as observed in the confocal images of MEF(10.1)Val5MycER cells; the three bands were present in the cytosolic fraction, whereas the upper band was nearly absent in the nucleus. With time, more cells entered apoptosis, and a progressive decrease was observed in the upper and middle cytosolic bands. At the same time, the nuclear fraction showed a clear increase in the lower band and a decrease in the middle band. These results suggest that the cytosolic form of DIO-1 is phosphorylated on serine/threonine and is predominant in healthy cells, whereas the unphosphorylated nuclear form is found under apoptotic conditions.

DIO-1 overexpression upregulates procaspase levels, leading to increased caspase activity. As discussed above, several lines of evidence suggest that nuclear translocation of DIO-1 is a step that activates the apoptotic machinery. Although the exact details of the programmed cell death pathways remain to be fully determined, the essential role of caspases at various stages of the apoptotic process has been established (3, 4, 38). The majority of apoptotic stimuli that signal through a pathway engage the common cell death machinery at the caspase level. We thus explored whether DIO-1 is also associated with caspase activation by examining procaspase levels and activity after transient expression of DIO-1 in FL5.12 cells.

Cells were initially treated with z-VAD-fmk to block proteolytic processing of the procaspases, facilitating accurate protein measurement in Western blot. Procaspases 3 and 9 were upregulated in wild-type cells induced to undergo apoptosis by IL-3 starvation. Similarly, DIO-1-transfected cells showed an increase in both proteins in the presence of IL-3, whereas transfection of the empty vector had no effect (Fig. 5A). In a fluorescence assay, protein lysates from cells not treated with caspase inhibitors were assayed for caspase activity. The previously observed increase in procaspase levels correlated with mature caspase activity (Fig. 5B). Caspase 3 showed an increase in activity following IL-3 starvation or DIO-1 expression compared to wild-type or mock-transfected cells. Caspases 6 and 9 were also activated, whereas caspase 2 showed lower activation levels. Caspase 8 was not implicated in IL-3-induced apoptosis and showed no variation after DIO-1 overexpression (not shown).

DIO-1ΔNLS is a dominant negative mutant that protects cells from apoptosis. To confirm that DIO-1 upregulates procaspases after its translocation to the nucleus, we performed similar experiments with the NLS deletion mutant, predicting failure to upregulate caspases due to its inability to translocate to the nucleus. We generated FL5.12 cells stably expressing DIO-1ΔNLS as well as a control bearing the empty vector. IL-3-starved empty vector cells showed procaspase 3 and 9 upregu-

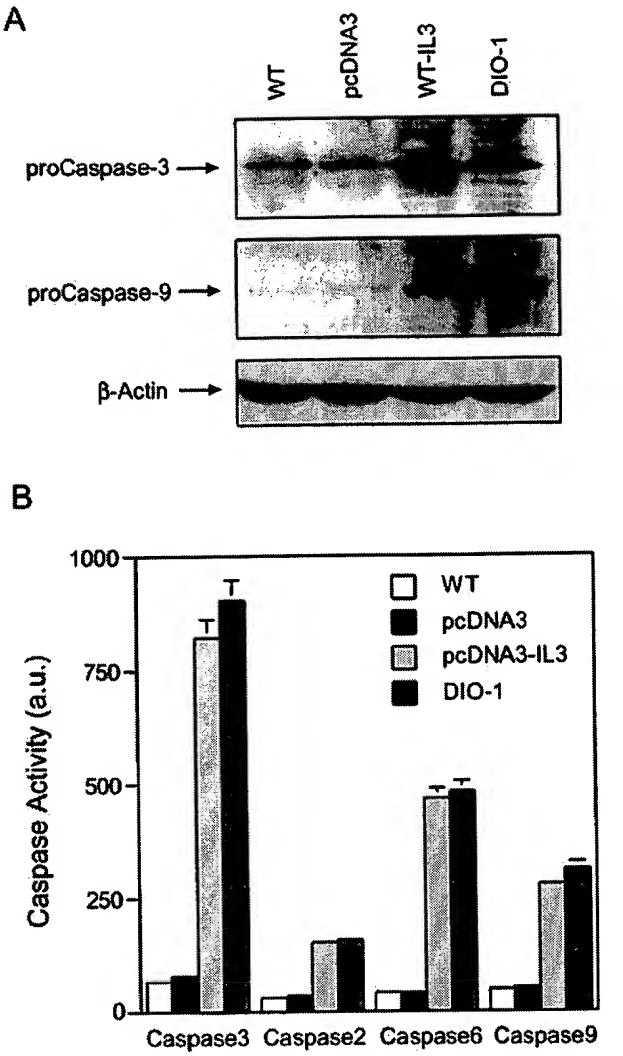

FIG. 5. DIO-1 upregulates and increases activation of caspases. (A) DIO-1 overexpression upregulates procaspase levels. FL5.12 cells were cultured in the presence of IL-3 (WT) or IL-3-starved for 24 h (WT-IL3). A plasmid vector (pcDNA3) or a DIO-1-expressing construct (DIO-1) were transiently transfected into FL5.12 cells and analyzed 24 h posttransfection. All cells were incubated with z-VAD-fmk (100 μM) to block proteolytic processing of the procaspase, facilitating accurate quantitation of protein levels. Procaspase 3 and 9 levels were analyzed in Western blots with anti-caspase 3 (upper panel) or anti-caspase 9 antibodies (middle panel). Loading was controlled with β-actin (lower panel). (B) Conditions as for panel A, but apoptosis was induced by IL-3 removal in pcDNA3-transiently transfected FL5.12 cells. Cells were cultured in the absence of z-VAD-fmk to measure caspase activity. Caspase 3-like, caspase 2, caspase 6, and caspase 9 activities were determined by fluorescence emission of the cleaved substrates (Materials and Methods). Data are given as the mean ± standard deviation for at least three independent experiments.

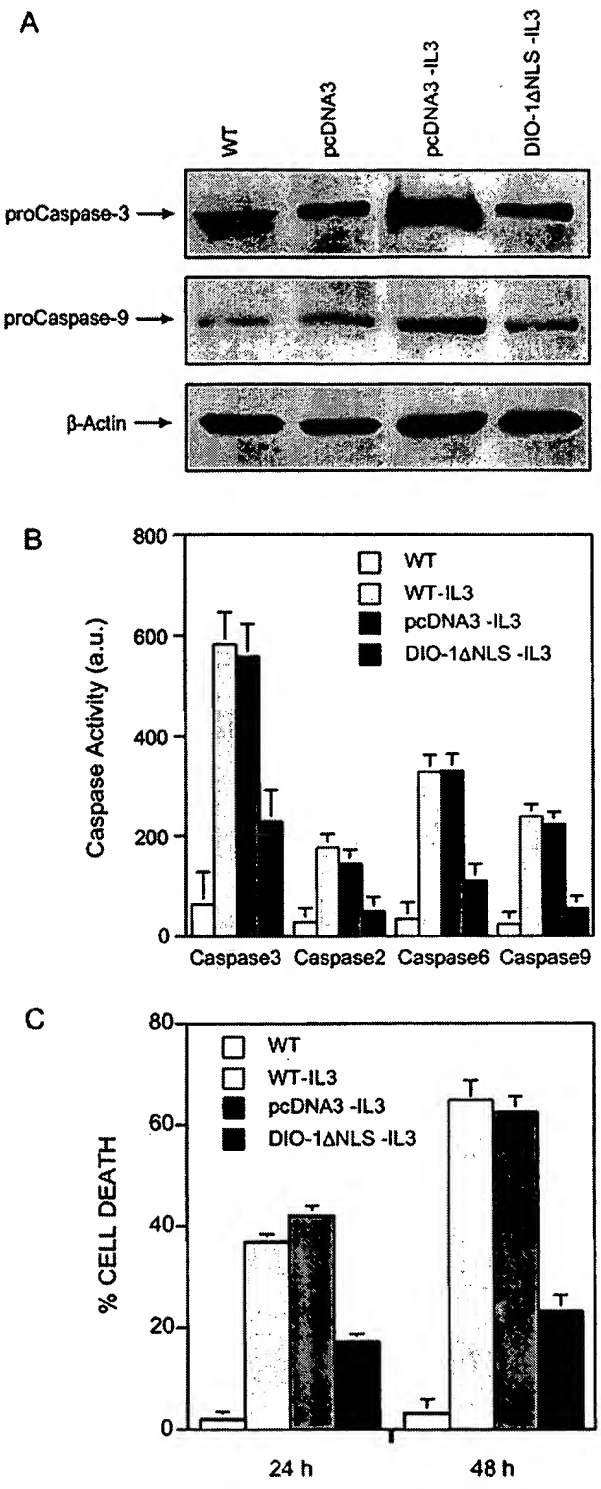

FIG. 6. DIO-1ΔNLS mutant is unable to upregulate and activate caspases. (A) FL5.12 cells were untreated (WT) or stably transfected with an empty vector (pcDNA3) or a DIO-1ΔNLS-expressing construct. Where indicated, IL-3 was removed from culture medium, and analysis was performed after 24 h. All cells were cultured in the presence of z-VAD-fmk (100 μM). Lysates were resolved by SDS-PAGE, followed by Western blotting with anti-caspase 3 (upper panel) or anti-caspase 9 (middle panel) antibodies. Loading was controlled with β-actin (lower panel). (B) Analysis of caspase activation. Samples were collected from FL5.12 wild-type (WT) cells cultured in the presence or absence of IL-3 and from the indicated stable FL5.12 cell lines in the absence of IL-3. Caspase activity was measured as in Fig. 5B. Results are expressed as the mean ± standard deviation for at least three independent experiments. a.u., arbitrary units. (C) DIO-1ΔNLS is a dominant negative mutant that protects cells from growth factor deprivation-induced apoptosis. FL5.12 wild-type cells (WT) and the FL5.12pcDNA3, and FL5.12DIO-1ΔNLS stable cell lines were induced to undergo apoptosis by IL-3 removal. Cells were collected at the times indicated, permeabilized, and propidium iodide stained (Materials and Methods). Apoptosis corresponds to the amount of fragmented DNA in the hypoploid sub-G_0/G_1 peak of the cell cycle. Values are expressed as percentages and represent the mean ± standard deviation for at least three independent experiments.

lation, whereas IL-3-starved cells expressing DIO-1ΔNLS did not upregulate procaspase levels (Fig. 6A). In addition, caspase activity in IL-3-starved DIO-1ΔNLS-expressing cells was clearly below the levels observed in DIO-1-transfected cells (Fig. 6B; compare to Fig. 5B). These low activity levels remained constant even after 48 h of IL-3 deprivation, when more than 60% of wild-type cells were apoptotic (not shown). The mutation thus failed to alter basal caspase levels. Taken together, these data suggest that DIO-1 translocation to the nucleus is essential to induce upregulation of several procaspases, to increase their activity, and to trigger the apoptotic pathway.

Given that the NLS mutation does not alter caspase levels, we tested whether it prevents apoptosis. FL5.12 wild-type cells were IL-3 starved, and apoptosis was measured by propidium iodide staining at 24 and 48 h postinduction (Fig. 6C). The cells underwent apoptotic cell death that increased with time, and similar results were obtained in FL5.12 pcDNA3 cells after IL-3 withdrawal. When FL5.12 cells stably expressing DIO-1ΔNLS (FL5.12 DIO-1ΔNLS) were IL-3 starved, we observed protection from apoptosis even after 48 h without the survival factor, with a reduction in the percentage of apoptotic cells of approximately 50% at 24 h and 66% at 48 h compared to cells expressing the empty vector. This behavior corresponds to a dominant negative mutation that is able to block the apoptotic signal transmitted by the wild-type form.

DISCUSSION

We report that DIO-1 translocation from the cytoplasm to the nucleus is an important early event in activating the apoptotic machinery. DIO-1 is present in the cell in multiple forms, which can be distinguished on the basis of their electrophoretic mobilities and their distinct subcellular localizations. We previously showed that DIO-1 mRNA and protein levels were upregulated by serum withdrawal from MEF(10.1)Val5MycER cells independently of p53-induced apoptosis (9). Here we show that, in the same cell system and with the same apoptotic stimulus, the DIO-1 gene product translocated to the nuclear compartment, whereas p53-induced cell death did not provoke alterations in its subcellular localization. The DIO-1 mutant lacking both NLSs (DIO-1ΔNLS) was unable to translocate to the nucleus or to trigger apoptosis, even in the presence of physiological death signals, and prevented IL-3 deprivation-induced cell death. The obser-

vation that DIO-1 but not DIO-1ΔNLS overexpression upregulated procaspase 3 and 9 levels and increased the activity of their mature forms establishes a link between the increase in DIO-1 levels and apoptosis induction (9). Although transcriptional activation by DIO-1 remains to be demonstrated, the need for nuclear translocation suggests that DIO-1 acts through the induction of caspase promoters rather than exerting a direct effect on cytoplasmic caspases. These findings are consistent with earlier studies reporting that transcriptional activation of caspases may be an important regulatory mechanism in programmed cell death (6, 12, 22, 29, 40).

One important model for caspase 9 activation involves its recruitment to Apaf-1 in the presence of ATP or dATP, following cytochrome *c* release from mitochondria (19, 42). Other authors propose that caspase 9 is activated and apoptosis can take place in the absence of cytochrome *c* (5, 10, 20, 32) after overexpression of the adaptor molecule Apaf-1 (16, 28), Nod-1 (14), TMS-1 (26), or CED-4 (35, 41). Furthermore, Apaf-1 mutants lacking the WD-40 repeats (WDR) constitutively self-associate and activate procaspase 9 independently of cytochrome *c* and dATP (13, 37). The *Caenorhabditis elegans* Apaf-1 homolog CED-4 lacks the WDR, implying that it may constitutively activate the procaspase 9 homolog CED-3 and suggesting that cytochrome *c* may not be required for CED-4-mediated CED-3 activation.

In our system, apoptosis induction via a DIO-1-triggered increase in procaspase 9 levels concurs with previous reports that procaspase 9 overexpression in vivo results in cell death, overriding the need for cytosolic cytochrome *c* (2, 14, 37). We observed that in MEF(10.1)Val5MycER and FL5.12 cells induced to apoptosis as well as in DIO-1-transfected cells, cytochrome *c* release was preceded by DIO-1 nuclear translocation and caspase upregulation (not shown). Caspase 9 activation is thus mediated by dimerization, and cytochrome *c*-induced recruitment by Apaf-1 creates high local caspase 9 concentrations that allow dimer-induced activation (31). This explains the caspase 9 activation observed prior to cytochrome *c* release from mitochondria.

Change in subcellular distribution is an important regulatory event for many proteins involved in apoptosis, cell cycle, or transcriptional regulation. Here we show that DIO-1 also changes its localization early in apoptosis induction and that this change is accompanied by an electrophoretic mobility shift. Nonetheless, the exact nature of the signal leading to these changes remains to be established. Coprecipitation of differentially tagged proteins showed that DIO-1 forms homo-oligomers in vivo. As homo-oligomers were detected for all forms, the oligomerization state is unlikely to differ following DIO-1 translocation to the nucleus. This has also been found for p53, which appears to be transported across the nuclear membrane in a tetrameric form (11). Proteolytic processing can also be ruled out as a regulatory mechanism, since all forms were detected with tags on either end of the protein. Although only the forms with lower electrophoretic mobility appeared to be phosphorylated, phosphorylation alone is not the basis of the mobility change. Additional modifications may thus be needed for the change in DIO-1 localization. In a similar case, MDM-2-mediated nuclear export of p53 depends on multiple signals that include the DNA-binding domain, conformational change, and C-terminal ubiquitination (11, 24); ubiquitinated p53 is subsequently degraded by proteasomes in the cytosol. DIO-1 localization may be regulated in a similar fashion. DIO-1 would thus be continuously modified and exported from the nucleus in healthy cells, appearing as cytosolic localization. In apoptotic cells, loss of the export signal would result in a net accumulation of the unmodified product in the nucleus.

DIO-1-mediated apoptosis requires caspase activation. In these experiments, neither procaspase upregulation nor caspase activation was detected after DIO-1ΔNLS overexpression, indicating that this mutant acts in a dominant negative manner, since it inhibits IL-3 withdrawal-induced apoptosis. This allows us to propose a model that explains the mechanism of DIO-1 activation and induction of cell death. In healthy cells, the DIO-1 transcript and protein are expressed at low basal levels, and the protein is found in the cytosol. Following an appropriate apoptotic stimulus, such as IL-3 starvation or c-*myc* induction in serum-free conditions, DIO-1 translocates to the nucleus before the appearance of any classical indicators of apoptotic machinery activation, such as caspase activation, alteration of cell membrane polarity, nuclear disruption, or DNA laddering. This indicates that DIO-1 activation is a very early step in apoptosis induction.

In our model, the presence of DIO-1 in the nucleus leads to an increase in procaspase 3 and 9 levels, resulting in caspase 9 activation. Activated caspase 9 can then activate procaspase 3. The processing of the large amounts of procaspase 3 gives rise to rapid accumulation of mature caspase 3, which acts as another amplification step due to caspase 3 feedback onto procaspase 9 Asp-330 (37). Subsequent cytochrome *c* release from mitochondria would induce Apaf-1 oligomerization, amplifying the apoptotic signal. The DIO-1ΔNLS mutant could form stable oligomers with wild-type DIO-1 and block nuclear translocation of the entire complex, preventing DIO-1-mediated gene upregulation and inhibiting the cell death program.

ACKNOWLEDGMENTS

We thank B. B. Wolf, D. R. Green, T. W. Mak, and R. Hakem for generous gifts of reagents, A. Ruiz-Vela for excellent and continuous advice, and A. Fütterer and M. Torres, A. Ruiz-Vela, K. van Wely, and M. Campanero for critical reading of the manuscript. We also thank I. López-Vidriero and M. C. Moreno-Ortiz for help with flow cytometry, all technical members of the department who aided with cell culture and general reagents, and C. Mark for editorial assistance.

D.G.D. is the recipient of a fellowship from the Spanish Ministerio de Educación y Ciencia. This work was supported by grants from the Ministerio de Ciencia y Tecnología and the European Union (QLG1-CT-2001-01536). The Department of Immunology and Oncology was founded and is supported by the Spanish Council for Scientific Research (CSIC) and the Pharmacia Corporation.

REFERENCES

1. **Alnemri, E. S., D. J. Livingston, D. W. Nicholson, G. Salvesen, N. A. Thornberry, W. W. Wong, and J. Yuan.** 1996. Human ICE/CED-3 protease nomenclature. Cell **87**:171.
2. **Bertin, J., W. J. Nir, C. M. Fischer, O. V. Tayber, P. R. Errada, J. R. Grant, J. J. Keilty, M. L. Gosselin, K. E. Robison, G. H. Wong, M. A. Glucksmann, and P. S. DiStefano.** 1999. Human CARD4 protein is a novel CED-4/Apaf-1 cell death family member that activates NF-κB. J. Biol. Chem. **274**:12955–12958.
3. **Boldin, M. P., T. M. Goncharov, Y. V. Goltsev, and D. Wallach.** 1996. Involvement of MACH, a novel MORT1/FADD-interacting protease, in Fas/APO-1- and TNF receptor-induced cell death. Cell **85**:803–815.
4. **Budihardjo, I., H. Oliver, M. Lutter, X. Luo, and X. Wang.** 1999. Biochemical pathways of caspase activation during apoptosis. Annu. Rev. Cell Dev. Biol. **15**:269–290.

5. **Chauhan, D., T. Hideshima, S. Rosen, J. C. Reed, S. Kharbanda, and K. C. Anderson.** 2001. Apaf-1/cytochrome *c*-independent and Smac-dependent induction of apoptosis in multiple myeloma (MM) cells. J. Biol. Chem. **276:** 24453–24456.
6. **Dai, C., and S. B. Krantz.** 1999. Interferon gamma induces upregulation and activation of caspases 1, 3, and 8 to produce apoptosis in human erythroid progenitor cells. Blood **93:**3309–3316.
7. **Earnshaw, W. C., L. M. Martins, and S. H. Kaufmann.** 1999. Mammalian caspases: structure, activation, substrates, and functions during apoptosis. Annu. Rev. Biochem. **68:**383–424.
8. **Ellis, R. E., J. Y. Yuan, and H. R. Horvitz.** 1991. Mechanisms and functions of cell death. Annu. Rev. Cell Biol. **7:**663–698.
9. **Garcia-Domingo, D., E. Leonardo, A. Grandien, P. Martinez, J. P. Albar, J. C. Izpisua-Belmonte, and C. Martinez-A.** 1999. DIO-1 is a gene involved in onset of apoptosis *in vitro*, whose misexpression disrupts limb development. Proc. Natl. Acad. Sci. USA **96:**7992–7997.
10. **Gross, A., J. Jockel, M. C. Wei, and S. J. Korsmeyer.** 1998. Enforced dimerization of BAX results in its translocation, mitochondrial dysfunction and apoptosis. EMBO J. **17:**3878–3885.
11. **Gu, J., L. Nie, D. Wiederschain, and Z. M. Yuan.** 2001. Identification of p53 sequence elements that are required for MDM2-mediated nuclear export. Mol. Cell. Biol. **21:**8533–8546.
12. **Gupta, S., V. Radha, Y. Furukawa, and G. Swarup.** 2001. Direct transcriptional activation of human caspase-1 by tumor suppressor p53. J. Biol. Chem. **276:**10585–10588.
13. **Hu, Y., M. A. Benedict, L. Ding, and G. Nuñez.** 1999. Role of cytochrome *c* and dATP/ATP hydrolysis in Apaf-1-mediated caspase-9 activation and apoptosis. EMBO J. **18:**3586–3595.
14. **Inohara, N., T. Koseki, L. del Peso, Y. Hu, C. Yee, S. Chen, R. Carrio, J. Merino, D. Liu, J. Ni, and G. Nuñez.** 1999. Nod1, an Apaf-1-like activator of caspase-9 and nuclear factor-κB. J. Biol. Chem. **274:**14560–14567.
15. **Jacobson, M. D., M. Weil, and M. C. Raff.** 1997. Programmed cell death in animal development. Cell **88:**347–354.
16. **Kamarajan, P., N. K. Sun, C. L. Sun, and C. C. Chao.** 2001. Apaf-1 overexpression partially overcomes apoptotic resistance in a cisplatin-selected HeLa cell line. FEBS Lett. **505:**206–212.
17. **Kerr, J. F., A. H. Wyllie, and A. R. Currie.** 1972. Apoptosis: a basic biological phenomenon with wide-ranging implications in tissue kinetics. Br. J. Cancer **26:**239–257.
18. **Li, H., H. Zhu, C. J. Xu, and J. Yuan.** 1998. Cleavage of BID by caspase 8 mediates the mitochondrial damage in the Fas pathway of apoptosis. Cell **94:**491–501.
19. **Li, P., D. Nijhawan, I. Budihardjo, S. M. Srinivasula, M. Ahmad, E. S. Alnemri, and X. Wang.** 1997. cytochrome *c* and dATP-dependent formation of Apaf-1/caspase-9 complex initiates an apoptotic protease cascade. Cell **91:**479–489.
20. **Li, P. F., R. Dietz, and R. von Harsdorf.** 1999. p53 regulates mitochondrial membrane potential through reactive oxygen species and induces cytochrome *c*-independent apoptosis blocked by Bcl-2. EMBO J. **18:**6027–6036.
21. **Liang, P., and A. B. Pardee.** 1992. Differential display of eukaryotic messenger RNA by means of the polymerase chain reaction. Science **257:**967–971.
22. **Liu, W., G. Wang, and A. G. Yakovlev.** 2002. Identification and functional analysis of the rat caspase-3 gene promoter. J. Biol. Chem. **277:**8273–8278.
23. **Liu, X., C. N. Kim, J. Yang, R. Jemmerson, and X. Wang.** 1996. Induction of apoptotic program in cell-free extracts: requirement for dATP and cytochrome *c*. Cell **86:**147–157.
24. **Lohrum, M. A., D. B. Woods, R. L. Ludwig, E. Balint, and K. H. Vousden.** 2001. C-terminal ubiquitination of p53 contributes to nuclear export. Mol. Cell. Biol. **21:**8521–8532.
25. **Luo, X., I. Budihardjo, H. Zou, C. Slaughter, and X. Wang.** 1998. Bid, a Bcl2 interacting protein, mediates cytochrome *c* release from mitochondria in response to activation of cell surface death receptors. Cell **94:**481–490.
26. **McConnell, B. B., and P. M. Vertino.** 2000. Activation of a caspase-9-mediated apoptotic pathway by subcellular redistribution of the novel caspase recruitment domain protein TMS1. Cancer Res. **60:**6243–6247.
27. **Muzio, M., A. M. Chinnaiyan, F. C. Kischkel, K. O'Rourke, A. Shevchenko, J. Ni, C. Scaffidi, J. D. Bretz, M. Zhang, R. Gentz, M. Mann, P. H. Krammer, M. E. Peter, and V. M. Dixit.** 1996. FLICE, a novel FADD-homologous ICE/CED-3-like protease, is recruited to the CD95 (Fas/APO-1) death-inducing signaling complex. Cell **85:**817–827.
28. **Perkins, C., C. N. Kim, G. Fang, and K. N. Bhalla.** 1998. Overexpression of Apaf-1 promotes apoptosis of untreated and paclitaxel- or etoposide-treated HL-60 cells. Cancer Res. **58:**4561–4566.
29. **Pohl, D., P. Bittigau, M. J. Ishimaru, D. Stadthaus, C. Hubner, J. W. Olney, L. Turski, and C. Ikonomidou.** 1999. *N*-Methyl-D-aspartate antagonists and apoptotic cell death triggered by head trauma in developing rat brain. Proc. Natl. Acad. Sci. USA **96:**2508–2513.
30. **Raff, M.** 1998. Cell suicide for beginners. Nature **396:**119–122.
31. **Renatus, M., H. R. Stennicke, F. L. Scott, R. C. Liddington, and G. S. Salvesen.** 2001. Dimer formation drives the activation of the cell death protease caspase 9. Proc. Natl. Acad. Sci. USA **98:**14250–14255.
32. **Ruiz-Vela, A., G. Gonzalez de Buitrago, and C. Martinez-A.** 1999. Implication of calpain in caspase activation during B cell clonal deletion. EMBO J. **18:**4988–4998.
33. **Salvesen, G. S., and V. M. Dixit.** 1999. Caspase activation: the induced-proximity model. Proc. Natl. Acad. Sci. USA **96:**10964–10967.
34. **Salvesen, G. S., and V. M. Dixit.** 1997. Caspases: intracellular signaling by proteolysis. Cell **91:**443–446.
35. **Shaham, S., and H. R. Horvitz.** 1996. Developing *Caenorhabditis elegans* neurons may contain both cell-death protective and killer activities. Genes Dev. **10:**578–591.
36. **Smith, P. K., R. I. Krohn, G. T. Hermanson, A. K. Mallia, F. H. Gartner, M. D. Provenzano, E. K. Fujimoto, N. M. Goeke, B. J. Olson, and D. C. Klenk.** 1985. Measurement of protein with bicinchoninic acid. Anal. Biochem. **150:**76–85.
37. **Srinivasula, S. M., M. Ahmad, T. Fernandes-Alnemri, and E. S. Alnemri.** 1998. Autoactivation of procaspase-9 by Apaf-1-mediated oligomerization. Mol. Cell **1:**949–957.
38. **Thornberry, N. A., and Y. Lazebnik.** 1998. Caspases: enemies within. Science **281:**1312–1316.
39. **Wolf, B. B., J. C. Goldstein, H. R. Stennicke, H. Beere, G. P. Amarante-Mendes, G. S. Salvesen, and D. R. Green.** 1999. Calpain functions in a caspase-independent manner to promote apoptosis-like events during platelet activation. Blood **94:**1683–1692.
40. **Yakovlev, A. G., K. Ota, G. Wang, V. Movsesyan, W. L. Bao, K. Yoshihara, and A. I. Faden.** 2001. Differential expression of apoptotic protease-activating factor-1 and caspase-3 genes and susceptibility to apoptosis during brain development and after traumatic brain injury. J. Neurosci. **21:**7439–7446.
41. **Yuan, J., and H. R. Horvitz.** 1992. The *Caenorhabditis elegans* cell death gene CED-4 encodes a novel protein and is expressed during the period of extensive programmed cell death. Development **116:**309–320.
42. **Zou, H., W. J. Henzel, X. Liu, A. Lutschg, and X. Wang.** 1997. Apaf-1, a human protein homologous to *C. elegans* CED-4, participates in cytochrome *c*-dependent activation of caspase-3. Cell **90:**405–413.